BioRisk 18: 57–91 (2022)
doi: 10.3897/biorisk.18.77001
https://biorisk.pensoft.net

RESEARCH ARTICLE

A peer-reviewed open-access journal
BioRisk

Potential risk resulting from the influence of static magnetic field upon living organisms. Numerically-simulated effects of the static magnetic field upon carbohydrates

Wojciech Ciesielski[1], Tomasz Girek[1], Henryk Kołoczek[2], Zdzisław Oszczęda[3], Jacek A. Soroka[4], Piotr Tomasik[3]

1 *Institute of Chemistry, Jan Długosz University, 42 201 Częstochowa, Poland* **2** *Institute of Chemistry and Inorganic Technology, Krakow University of Technology, 31155 Krakow, Poland* **3** *Nantes Nanotechnological Systems, 59 700 Bolesławiec, Poland* **4** *Scientific Society of Szczecin, 71-481 Szczecin, Poland*

Corresponding author: Wojciech Ciesielski (w.ciesielski@interia.pl)

Academic editor: Josef Settele | Received 24 October 2021 | Accepted 3 April 2022 | Published 6 June 2022

Citation: Ciesielski W, Girek T, Kołoczek H, Oszczeda Z, Soroka JA, Tomasik P (2022) Potential risk resulting from the influence of static magnetic field upon living organisms. Numerically-simulated effects of the static magnetic field upon carbohydrates. BioRisk 18: 57–91. https://doi.org/10.3897/biorisk.18.77001

Abstract

Background: Recognising effects of static magnetic field (SMF) of varying flux density on flora and fauna is attempted. For this purpose, the influence of SMF upon molecules of *a*- and *β*-D-glucose, *a*- and *β*-D-galactose, *a*- and *β*-fructopyranoses, *a*- and *β*-fructofuranoses and *a*- and *β*-D-xylofuranoses and *a* and *β*-D-xylopyranoses is studied.

Methods: Computations of the effect of static magnetic field (SMF) of 0.0, 0.1, 1, 10 and 100 AFU (1 AFU > 1000 T) flux density were performed in silico for SMF changes distribution of the electron density in these molecules.

Hyper-Chem 8.0 software was used together with the AM1 method for optimisation of the conformation of the molecules of monosaccharides under study. Then polarisability, charge distribution, potential and dipole moment for molecules placed in SMF were calculated involving DFT 3-21G method.

Results: Application of SMF induced polarisability of electrons, atoms and dipoles, the latter resulting in eventual re-orientation of the molecules along the applied field of the molecules and the electron density redistribution at particular atoms. Increase in the field strength generated mostly irregular changes of the electron densities at particular atoms of the molecules as well as polarisabilities. Energy of these molecules and their dipole moments also varied with the SMF flux density applied.

Conclusions: Saccharides present in the living organisms may participate in the response of the living organisms to SMF affecting metabolism of the molecules in the body fluids by fitting molecules to the enzymes. Structural changes of saccharide components of the cell membranes can influence the membrane permeability.

Keywords
D-fructose, D-galactose, D-glucose, D-xylose, organisms, static magnetic field

Introduction

Carbohydrates (mono-, di-, oligo- and polysaccharides) serve several key functions in fauna and flora. Customarily, products of their physical, chemical and biological transformations are also accounted for in this group of compounds. Cellulose, a polysaccharide, is the most abundant carbohydrate all over the world. It is a structural component of the cell walls of plants including aquatic plants like algae. Green plants, which constitute about half of the living matter on the earth, also contain abundant number of mono-, di- and oligosaccharides. Some of them are found also in animals. Metabolism of those oligo- and lower carbohydrates provides energy and nutrients for the plants (Heldt and Piechulla 2010).

In organisms of fauna and their life, the role of carbohydrates is much more complex than in plants. They co-build membranes of body cells and microorganisms colonising the body, enzymes and elements of genetic code. Carbohydrates are present in systems protecting the cells from oxidative stress and participate in several reactions in the body (Maton et al. 1993; Campbell et al. 2006; Reynolds et al. 2019). Carbohydrates in various forms are delivered to the organisms as food components. The latter are either physically, chemically or enzymatically transformed (metabolised) or left intact playing the role of fibre. Fibre promotes a proper functioning of the excretory system and, as an adsorbent, removes toxins concentrated in the intestines. All kinds of physical, chemical and biochemical transformations are controlled by several factors, such as conformations of reacting molecules, equilibria, formation of transition molecule – enzyme transition states and mechanisms of the transformations which can be either reversible or irreversible. Their transformation can proceed following either ionic or radical mechanisms (Tomasik 1997; Tomasik 2007a, 2007b; Keung and Mehta 2015; Churuangsuk et al. 2018).

The effect of increasing environmental pollution with a magnetic field (Hamza et al. 2002; Rankovic and Radulovic 2009) and the role of the magnetic field in current and future technologies (Committee to Assess the Current Status and Future Direction of High Magnetic Field Science in the United States, Board on Physics and Astronomy 2013; Bao and Guo 2021; Tang et al. 2021) evokes certain anxiety. Therefore, recently (Ciesielski et al. 2021) we presented a numerically-simulated effect of static magnetic field (SMF) on the structure and behaviour of simple molecules, that is, triplet and singlet oxygen, nitrogen, water, ammonia, carbon dioxide and methane (Ciesielski et al. 2021) and lower alkanols (Ciesielski et al. 2022). The results prompted us to study the effect of that field upon further molecules important in constituting and functioning organisms of flora and fauna.

This paper presents results of numerical computations applied to selected monosaccharides, that is to *α*- and *β*-D-glucose, *α*- and *β*-D-galactose, *α*- and *β*-fructopyranoses, *α*- and *β*-fructofuranoses, *α*- and *β*-D-xylopyranoses and *α*- and *β*-D-xylofuranoses. They play essential roles in building structure and functioning of organisms of flora and fauna.

Numerical computations

Molecular structures were drawn using the Fujitsu SCIGRESS 2.0 software (Marchand et al. 2014). Their principal symmetry axes were orientated along the x-axis of the Cartesian system. A molecule of saccharide was situated inside of a triaxial elypsoid. The long axis of that ellipsoid was accepted to be the x-axis. The shortest axis quasi-perpendicular to either the pyranose or furanose ring was considered as the z-axis. The y-axis was quasi-parallel to those rings plane. The magnetic field was fixed in the same direction, along the x-axis with the south pole from the left side. Subsequently, involving Gaussian 0.9 software, equipped with the 6-31G** basis (Frisch et al. 2016) i.e. equipped with multiple polarization functions (Frisch et al. 1984), the molecules were optimised and all values of bond length, dipole moment, health of formation, bond energy and total energy for the systems were computed.

In the next step, the tendency of the static magnetic field (SMF) influence, employed as Arbitrary Field Unit (AFU) (1 AFU > 1000 T), upon optimised molecules was computed with Amsterdam Modelling Suite software (Farberovich and Mazalova 2016; Charistos and Muñoz-Castro 2019) and the NR_LDOTB (non-relativistically orbital momentum L-dot-B) method (Glendening et al. 1987; Carpenter and Weinhold 1988). Following that step, values of bond length, dipole moment, health of formation equal to the energy of dissociation and charges at the atoms, were calculated using Gaussian 0.9 software equipped with the 6-31G** basis (Frisch et al. 2016).

Visualisation of molecules in the coordinate system was performed involving the HyperChem 8.0 software (Froimowitz 1993).

Results

Numerical simulations were performed for both anomers of D-glucose (Fig. 1)

Both anomers of D-galactose (Fig. 2)

Both anomers of D-fructopyranoses and both anomers of D-fructofuranoeses (Fig. 3)

Both anomers of D-xylopyranoses and both anomers of D-xylofuranoses (Fig. 4)

Particular structures contain numbering atoms followed in further discussions.

Tables 1–3 provide data illustrating properties of the α- and β-D-glucose molecules situated along the x-axis of the Cartesian system in SMF of the flux density of 0 to 100 AFU, distribution of charge density and bond lengths in those molecules, respectively.

Results of those computations are visualised in Fig. 5.

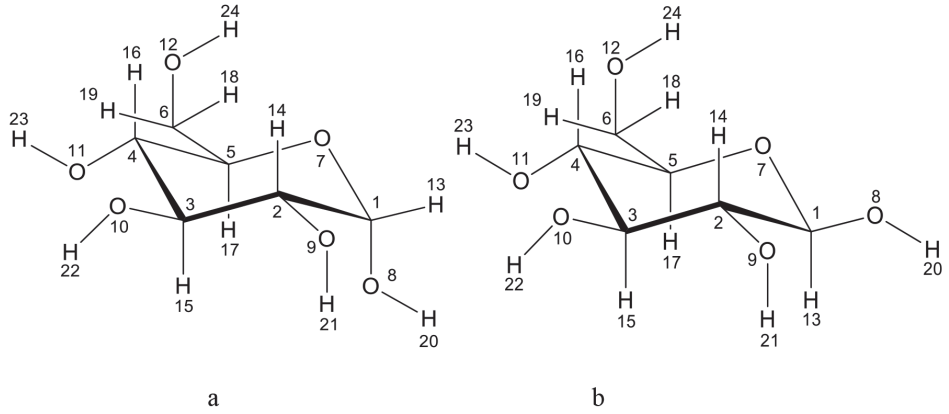

Figure 1. Structure of α- and β-D-glucose (**a** and **b** respectively) and followed by numbering of atoms.

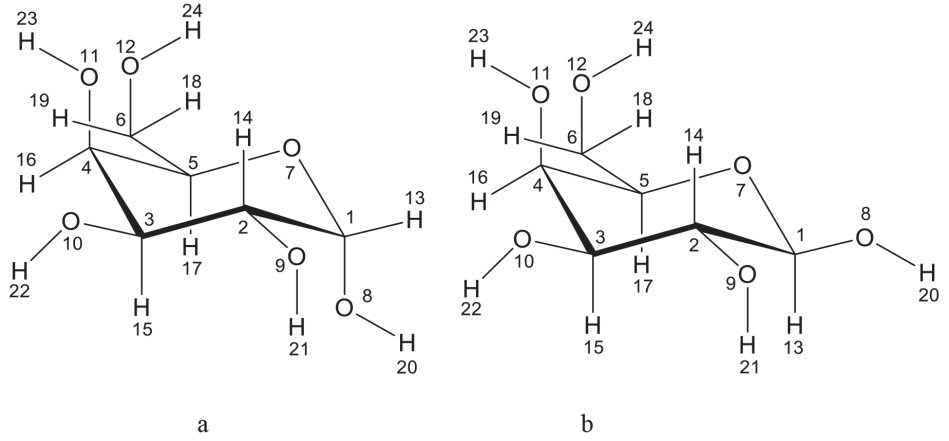

Figure 2. Structure of α- and β-D-galactose (**a** and **b** respectively) and followed by numbering of atoms.

Table 1. Properties of the α- and β-D-glucose molecules situated along the x-axis of the Cartesian system in SMF of the flux density of 0 to 100 AFU.

Property	Anomer	Flux density [AFU]				
		0	**0.1**	**1**	**10**	**100**
Dipole moment [D]	α	8.68	8.69	8.77	8.89	9.06
	β	8.34	8.44	9.75	10.12	14.52
Heat of formation [kcal/mole]	α	-1259.6	-1259.6	-1248.7	-1141.5	-985.8
	β	-1246.6	-1245.8	-1223.5	-1095.3	-912.6

Corresponding data computed for anomers of D-galactose are presented in Tables 4–6. They are visualised in Fig. 6.

Tables 7–9 contain results of analogous computations for anomers of D-fructopyranoses and visualisation of those data are visualised in Fig. 7.

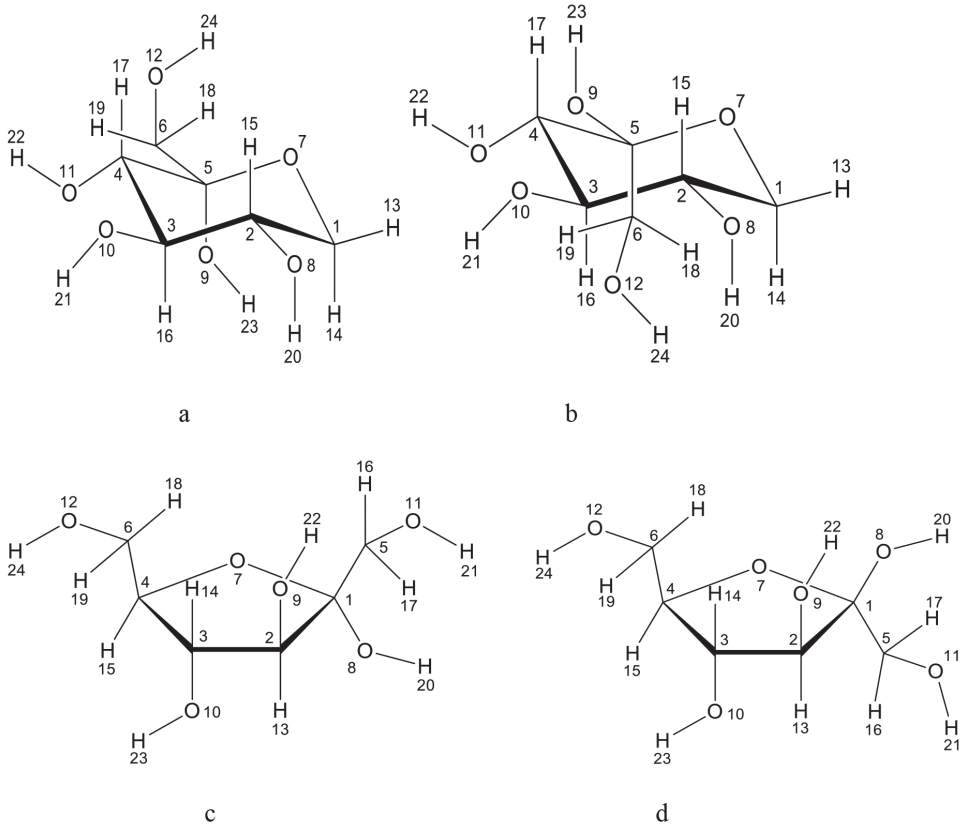

Figure 3. Structure of α- and β-D-fructopyranoses (**a** and **b** respectively) and α- and β-D-fructofuranoses (**c** and **d** respectively) and followed by numbering of atoms.

Properties computed for anomers of D-fructofuranoses are given in Tables 7, 10 and 11 and their visualisation can be seen in Fig. 8.

Corresponding data for D-xylopyranose anomers are provided in Tables 12–14 and visualisation of those data are presented in Fig. 9.

Finally, computations for anomers of D-xylofuranoses are presented in Tables 12, 15 and16. Visualisation of those data is given in Fig. 10.

Discussion

This study focused on recognising effects of SMF upon metabolism of monosaccharides in the organisms of fauna and flora. Particular attention was paid to the effect of SMF of increasing flux density upon the charge density at the atoms being the reaction sites of the selected monosaccharide molecules responsible for initiating the metabolic processes.

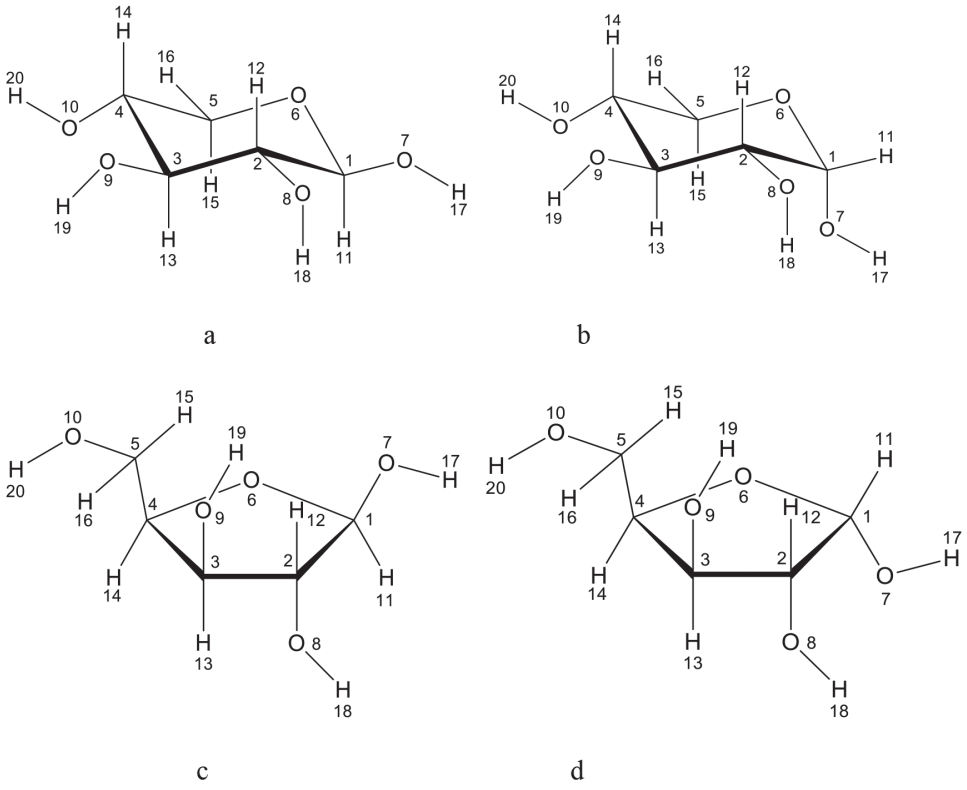

Figure 4. Structure of α- and β-D-xylopyranoses (**a** and **b** respectively) and α- and β-D-xylofuranoses (**c** and **d** respectively) and followed by numbering of atoms.

SMF could perturb the trajectory of bonds forming electrons involving the Lorentz force. Additionally, the stability of the lone and bonding electron pairs resulting from their oppositely-directed magnetic spins could be reduced. Such kind of electron pairs reside in valence bonds and in non-bonding lone electron pairs of the oxygen atoms. One of the two lone electron pairs of the latter atoms should be particularly sensitive to the effect of SMF. SMF could turn hybridisation of that atom from nearly sp^2 to sp^3 proportionally to an increase in the flux density. That effect would influence the electrostatic interactions through space within the molecules.

D-Glucose

This aldohexose resides chiefly in the cyclic form of α- and β-pyranose (Fig. 1). The thermodynamically less stable open-chain molecule spontaneously isomerises into one of two anomeric pyranoses (Tomasik 1997; Tomasik 2007a;, 2007b; Keung and Mehta 2015; Churuangsuk et al. 2018).

Both anomers of D-glucose, that is, α- and β-D-glucose are utilied in organisms of flora and fauna as a main source of energy (Domb et al. 2019). They are directly

Table 2. Charge density [a.u] at particular atoms of the α- and β-D-glucose molecules depending on SMF flux density [AFU].

Atom		Fluxdensity[AFU]				
	Tendency	0	0.1	1.0	10	100
C1	**H1**	**0.421**	**0.428**	**0.430**	**0.435**	**0.434**
	L2	***0.466***	***0.442***	***0.425***	***0.398***	***0.375***
C2	**H3**	**0.094**	**0.108**	**0.126**	**0.148**	**0.156**
	H2	***0.138***	***0.149***	***0.161***	***0.172***	***0.178***
C3	**V**	**0.135**	**0.137**	**0.129**	**0.050**	**0.053**
	V	***0.108***	***0.108***	***0.079***	***0.050***	***0.093***
C4	**V**	**0.176**	**0.179**	**0.181**	**0.153**	**0.164**
	L1	***0.192***	***0.192***	***0.187***	***0.166***	***0.163***
C5	**IL**	**0.121**	**0.121**	**0.124**	**0.076**	**0.067**
	IL	***0.102***	***0.110***	***0.096***	***0.058***	***0.034***
C6	**H3**	**0.004**	**0.010**	**0.036**	**0.371**	**0.427**
	H	***0.009***	***0.027***	***0.139***	***0.374***	***0.460***
O7	**IH**	**-0.639**	**-0.636**	**-0.632**	**-0.620**	**-0.628**
	H2	***-0.631***	***-0.620***	***-0.610***	***-0.598***	***-0.017***
O8	**L2**	**-0.697**	**-0.706**	**-0.715**	**-0.734**	**-0.736**
	H2	***-0.727***	***-0.708***	***-0.702***	***-0.696***	***-0.688***
O9	**IH**	**-0.706**	**-0.708**	**-0.708**	**-0.689**	**-0.683**
	H	***-0.752***	***-0.750***	***-0.740***	***-0.716***	***-0.696***
O10	**IH**	**-0.752**	**-0.745**	**-0.721**	**-0.475**	**-0.551**
	H2	***-0.745***	***-0.712***	***-0.580***	***-0.489***	***-0.634***
O11	**V**	**-0.744**	**-0.741**	**-0.738**	**-0.724**	**-0.740**
	V	***-0.747***	***-0.740***	***-0.735***	***-0.728***	***-0.753***
O12	V	-0.711	-0.715	-0.716	-0.669	-0.651
	H1	*-0.708*	*-0.707*	*-0.702*	*-0.659*	*-0.600*
H13	**V**	**0.174**	**0.173**	**0.172**	**0.184**	**0.187**
	V	***0.150***	***0.147***	***0.155***	***0.169***	***0.172***
H14	**L**	**0.182**	**0.178**	**0.175**	**0.174**	**0.175**
	V	***0.192***	***0.191***	***0.161***	***0.201***	***0.201***
H15	**IH**	**0.200**	**0.201**	**0.204**	**0.241**	**0.240**
	V	***0.155***	***0.153***	***0.164***	***0.172***	***0.134***
H16	**V**	**0.196**	**0.195**	**0.194**	**0.198**	**0.191**
	V	***0.207***	***0.207***	***0.207***	***0.211***	***0.205***
H17	IH	0.186	0.185	0.186	0.228	0.230
	H1	*0.161*	*0.162*	*0.179*	*0.214*	*0.221*
H18	L3	0.155	0.130	0.075	-0.479	-0.493
	L3	*0.156*	*0.093*	*-0.087*	*-0.488*	*-0.434*
H19	IH	0.186	0.183	0.185	0.256	0.278
	H2	*0.186*	*0.183*	*0.197*	*0.257*	*0.513*
H20	H1	0.406	0.409	0.412	0.438	0.439
	V	*0.415*	*0.410*	*0.408*	*0.415*	*0.408*
H21	V	0.395	0.396	0.393	0.393	0.396
	L1	*0.422*	*0.420*	*0.413*	*0.407*	*0.391*
H22	L3	0.405	0.396	0.370	0.120	0.087
	L2	*0.423*	*0.395*	*0.285*	*0.187*	*0.133*
H23	V	0.417	0.417	0.416	0.422	0.433
	V	*0.420*	*0.420*	*0.418*	*0.424*	*0.438*
H24	H2	0.395	0.407	0.421	0.502	0.523
	H2	*0.397*	*0.418*	*0.451*	*0.500*	*0.513*

[a]Data in normal font and in italics are for α- and β-anomers, respectively. Data given in bold are related to the effects at atoms which could be interpreted in details as not perturbed by a free rotation. Notation: H - high, L - low, IH and IL- irregular high and irregular low changes, respectively and V – totally irregular changes of the values. Figures following symbol or L characterise intensity of the change: 1 –weak, 2 – moderate, 3 – very strong.

Table 3. Bond lengths [Å] in the α- and β-D-glucose molecules depending on the applied SMF flux density [AFU][a].

Bond		Flux density [AFU]				
	Tendency	0	0.1	1	10	100
C1-C2	**H1**	**1.530**	**1.536**	**1.554**	**1.579**	**1.587**
	H1	***1.528***	***1.533***	***1.534***	***1.539***	***1.552***
C1-O8	**L1**	**1.413**	**1.413**	**1.408**	**1.389**	**1.394**
	L1	***1.390***	***1.389***	***1.387***	***1.382***	***1.382***
O8-H20	H1	0.972	1.011	1.048	1.041	1.045
	V	*0.972*	*1.058*	*1.020*	*1.062*	*1.028*
C1-H13	**H1**	**1.099**	**1.117**	**1.125**	**1.121**	**1.126**
	H1	***1.100***	***1.194***	***1.169***	***1.164***	***1.156***
C2-C3	**H1**	**1.528**	**1.530**	**1.533**	**1.553**	**1.561**
	H1	***1.526***	***1.532***	***1.545***	***1.552***	***1.547***
C2-O9	**H1**	**1.412**	**1.411**	**1.413**	**1.427**	**1.427**
	H1	***1.412***	***1.416***	***1.417***	***1.424***	***1.431***
O9-H21	V	0.972	1.007	1.004	1.004	0.993
	V	*0.972*	*0.989*	*0.983*	*0.955*	*0.969*
C2-H14	**H1**	**1.099**	**1.147**	**1.153**	**1.155**	**1.149**
	H1	***1.099***	***1.187***	***1.170***	***1.152***	***1.155***
C3-C4	**V**	**1.527**	**1.518**	**1.514**	**1.525**	**1.523**
	V	***1.527***	***1.514***	***1.517***	***1.530***	***1.534***
C3-O10	**V**	**1.412**	**1.416**	**1.423**	**1.381**	**1.397**
	V	***1.412***	***1.419***	***1.3934***	***1.378***	***1.194***
O10-H22	H3	0.972	1.198	1.389	3.084	3.685
	H3	*0.972*	*1.378*	*1.979*	*2.886*	*3.990*
C3-H15	**H1**	**1.099**	**1.115**	**1.132**	**1.127**	**1.134**
	H1	***1.099***	***1.132***	***1.116***	***1.148***	***1.125***
C4-C5	**V**	**1.533**	**1.529**	**1.531**	**1.529**	**1.525**
	V	***1.532***	***1.530***	***1.527***	***1.533***	***1.538***
C4-O11	**H1**	**1.412**	**1.422**	**1.434**	**1.461**	**1.476**
	H1	***1.412***	***1.427***	***1.442***	***1.455***	***1.461***
O11-H23	V	0.972	0.968	0.972	0.964	0.964
	V	*0.972*	*0.969*	*0.957*	*0.977*	*0.970*
C4-H16	**H2**	**1.099**	**1.161**	**1.169**	**1.176**	**1.171**
	H2	***1.099***	***1.187***	***1.168***	***1.140***	***1.153***
C5-C6	H1	1.528	1.531	1.540	1.556	1.570
	H1	*1.528*	*1.532*	*1.538*	*1.553*	*1.559*
C6-O12	IL	1.412	1.392	1.368	1.292	1.298
	IL	*1.412*	*1.375*	*1.328*	*1.287*	*1.309*
O12-H24	H	0.972	0.995	1.011	1.050	1.058
	H	*0.972*	*1.026*	*1.048*	*1.050*	*1.061*
C6-H18	H2	1.099	1.148	1.150	1.168	1.169
	V	*1.099*	*1.184*	*1.204*	*1.175*	*1.189*
C6-H19	H3	1.099	1.262	1.444	2.675	3.259
	H3	*1.099*	*1.410*	*1.771*	*2.656*	*3.742*
C5-O7	**V**	**1.433**	**1.431**	**1.429**	**1.429**	**1.437**
	V	***1.434***	***1.430***	***1.430***	***1.435***	***1.467***
O7-C1	**L1**	**1.433**	**1.414**	**1.392**	**1.387**	**1.375**
	V	***1.432***	***1.402***	***1.3942***	***1.400***	***1.403***

[a]See Table 2 for notation.

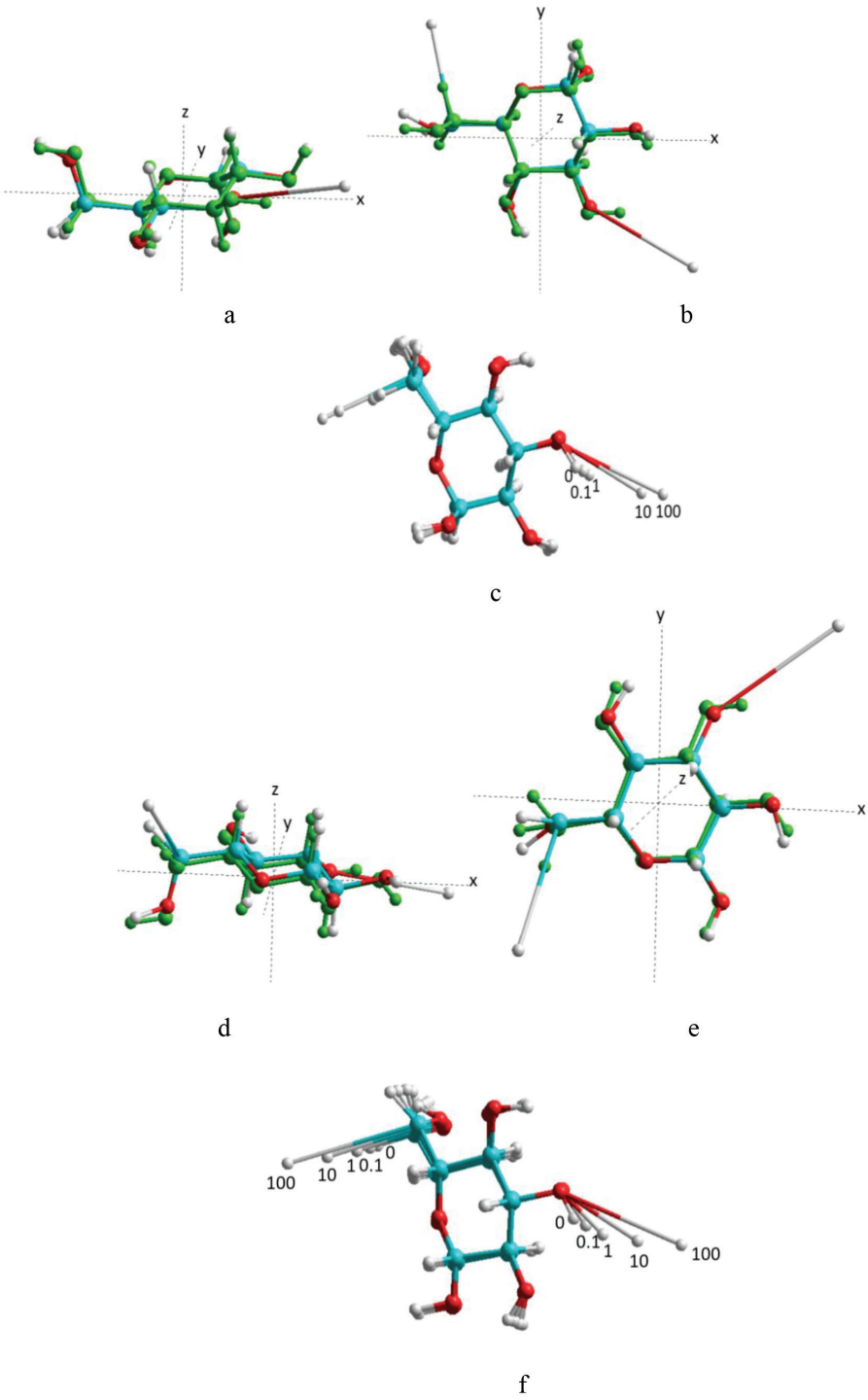

Figure 5. Simplified visualisation of the effect of SMF upon conformation and bond length of α-D- and β-D-glucose anomers (**a–c** and **d–f** respectively), situated in the Cartesian system.

Table 4. Properties of the α- and β-D-galactose molecules situated along the x-axis of the Cartesian system in SMF of the flux density of 0 to 100 AFU.

Property	Anomer	Flux density [AFU]				
		0	0.1	1	10	100
Dipole moment [D]	α	8.63	8.72	8.83	8.93	9.18
	β	8.66	8.72	8.88	8.98	9.32
Heat of formation [kcal/mole]	α	-1286.3	-1285.2	-1267.4	-1206.5	-1128.4
	β	-1252.3	-1251.2	-1247.4	-1198.7	-1111.3

metabolised in the body. In human organisms, that energy is generated chiefly from glycogen stored in the liver. Under specific cases, D-glucose is delivered into organisms as a component of food, for instance, a spice and supplement of diet injected as an additional source of energy (World Health Organization 2019). D-Glucose is metabolised in enzymatic processes. The first step of that process involves its esterification with adenosine-triphosphate (ATP) at the C6-OH group (Heinrich et al. 2014). Within the Entner-Doudoroff pathway operating in Gram-negative bacteria, certain Gram-positive bacteria and archaea begin at the same reaction site engaging the C1 atom (Conway 1992).

One of the important enzymatic reactions of D-glucose, called the Maillard reaction, is known as the enzymatic browning reaction. In the reaction of D-glucose with lysine and arginine, residues of the protein pentosidine are formed (Sell and Monnier 1989). Pentosidine is formed most readily from pentoses, but glucose, fructose and other saccharides may also react in such a manner.

Performed computations showed that, based on the criterion of heat of formation, the α-D-anomer was slightly more stable than the β-D-anomer (Table 1). The stability of both anomers decreased unevenly against the applied SMF flux density. The β-D-anomer reacted more strongly to SMF. It was also associated with a significantly stronger increase in dipole moment. These trends fitted results performed with density functional/*ab initio* computation in silico. The same computations for both anomers of D-glucose in water pointed to the α-D-anomer as more stable than the β-D-anomer (Facundo Ruiz et al. 2005). However, electrochemical oxidation of the α-D-anomer glucose and β-D-anomer on the anode surface showed that the β-D-anomer was much more reactive (Largeaud et al. 1995).

The charge density at particular atoms of both anomers varied irregularly with an increase in the flux density (Table 2). An increase in the SMF flux density produced a more remarkable decrease in the electron density at the 1,2,4,5,6,7,11,12,15 and 20 atoms of the β-anomer than at the same atoms of the α-anomer. Extremely strong, but an opposite effect was noted at the C2 and H21 atoms. Both atoms were bound to one another and the C2 atom was in the vicinity to the endocyclic O7 atom. Thus, observed effects could result from electrostatic interactions through space involving a partially weakened lone electron pair of the oxygen atom. An increase in the electron density produced by SMF was observed at C1β (atom C1, β-anomer), C4β, C5, O8α and H14α atoms, whereas the electron density remarkably decreased at C1α, C2, O7α,

Table 5. Charge density [a.u] at particular atoms of the α- and β-D-glucose molecules depending on SMF flux density [AFU].

Atom		Flux density [AFU]				
	Tendency	0	0.1	1.0	10	100
C1	**V**	**0.447**	**0.456**	**0.452**	**0.439**	**0.399**
	V	***0.448***	***0.436***	***0.426***	***0.431***	***0.398***
C2	**H1**	**0.112**	**0.113**	**0.132**	**0.148**	**0.203**
	IH	***0.191***	***0.197***	***0.200***	***0.185***	***0.210***
C3	**IL**	**0.102**	**0.131**	**0.086**	**0.040**	**0.099**
	L1	***0.112***	***0.111***	***0.090***	***0.045***	***0.077***
C4	**IH**	**0.086**	**0.094**	**0.108**	**0.114**	**0.105**
	V	***0.118***	***0.125***	***0.128***	***0.128***	***0.107***
C5	**L2**	**0.129**	**0.129**	**0.027**	**-0.044**	**-0.112**
	IL	***0.107***	***0.112***	***0.080***	***0.002***	***-0.069***
C6	**H2**	**-0.038**	**-0.043**	**0.212**	**0.310**	**0.483**
	H2	***-0.040***	***-0.062***	***0.001***	***0.249***	***0.476***
O7	**V**	**-0.641**	**-0.641**	**-0.645**	**-0.637**	**-0.641**
	IL	***-0.629***	***-0.626***	***-0.622***	***-0.612***	***-0.623***
O8	**IL**	**-0.714**	**-0.734**	**-0.749**	**-0.749**	**-0.745**
	H1	***-0.698***	***-0.688***	***-0.669***	***-0.668***	***-0.646***
O9	**V**	**-0.747**	**-0.746**	**-0.745**	**-0.742**	**-0.772**
	V	***-0.728***	***-0.721***	***-0.713***	***-0.700***	***-0.733***
O10	**V**	**-0.747**	**-0.758**	**-0.607**	**-0.502**	**-0.712**
	V	***-0.719***	***-0.706***	***-0.665***	***-0.483***	***-0.692***
O11	**H1**	**-0.777**	**-0.769**	**-0.731**	**-0.679**	**-0.608**
	H1	***-0.690***	***-0.685***	***-0.667***	***-0.660***	***-0.617***
O12	H	-0.758	-0.727	-0.677	-0.619	-0.534
	H	*-0.724*	*-0.704*	*-0.674*	*-0.628*	*0.551*
H13	**V**	**0.183**	**0.184**	**0.184**	**0.195**	**0.181**
	V	***0.156***	***0.146***	***0.144***	***0.150***	***0.163***
H14	**V**	**0.190**	**0.181**	**0.182**	**0.190**	**0.183**
	V	***0.220***	***0.219***	***0.218***	***0.228***	***0.210***
H15	**V**	**0.196**	**0.202**	**0.217**	**0.233**	**0.150**
	V	***0.167***	***0.167***	***0.170***	***0.183***	***0.110***
H16	**V**	**0.189**	**0.195**	**0.205**	**0.214**	**0.200**
	H1	***0.185***	***0.186***	***0.192***	***0.205***	***0.209***
H17	**IH**	**0.204**	**0.233**	**0.302**	**0.354**	**0.353**
	H1	***0.174***	***0.179***	***0.195***	***0.236***	***0.267***
H18	H1	0.205	0.204	0.239	0.283	0.301
	IH	*0.182*	*0.166*	*0.169*	*0.214*	*0.283*
H19	L2	0.181	0.093	-0.277	-0.496	-0.315
	L2	*0.163*	*0.158*	*0.040*	*-0.349*	*-0.376*
H20	H1	0.431	0.436	0.443	0.451	0.457
	V	*0.395*	*0.396*	*0.394*	*0.408*	*0.388*
H21	V	0.435	0.433	0.422	0.423	0.434
	H1	*0.411*	*0.412*	*0.412*	*0.413*	*0.420*
H22	IL	0.445	0.449	0.443	0.209	0.078
	IL	*0.394*	*0.379*	*0.339*	*0.179*	*0.105*
H23	L1	0.461	0.446	0.414	0.384	0.325
	L1	*0.398*	*0.394*	*0.382*	*0.374*	*0.339*
H24	H1	0.425	0.438	0.455	0.480	0.487
	H1	*0.409*	*0.411*	*0.427*	*0.472*	*0.524*

[a]See Table 2 for notation.

Table 6. Bond lengths [Å] in the α- and β-D-galactose molecules depending on the applied SMF flux density [AFU][a].

Bond	Tendency	Flux density [AFU]				
		0	0.1	1	10	100
C1-C2	**V**	**1.5120**	**1.528**	**1.551**	**1.542**	**1.551**
	V	***1.540***	***1.543***	***1.560***	***1.556***	***1.551***
C1-O8	**V**	**1.404**	**1.412**	**1.110**	**1.411**	**1.401**
	V	***1.430***	***1.421***	***1.400***	***1.388***	***1.366***
O8-H20	V	0.978	0.974	0.962	0.974	0.966
	IH	*0.960*	*1.011*	*1.071*	*1.026*	*1.096*
C1-H13	**V**	**1.100**	**1.141**	**1.103**	**1.149**	**1.116**
	V	***1.090***	***1.179***	***1.168***	***1.172***	***1.092***
C2-C3	**V**	**1.515**	**1.497**	**1.504**	**1.576**	**1.536**
	V	***1.537***	***1.520***	***1.505***	***1.510***	***1.543***
C2-O9	**V**	**1.408**	**1.390**	**1.386**	**1.390**	**1.410**
	IL	***1.430***	***1.416***	***1.394***	***1.386***	***1.424***
O9-H21	V	0.979	1.003	0.962	0.991	0.955
	V	*0.960*	*1.013*	*1.014*	*0.998*	*0.972*
C2-H14	**V**	**1.100**	**1.189**	**1.171**	**1.212**	**1.166**
	IH	***1.090***	***1.137***	***1.171***	***1.180***	***1.159***
C3-C4	**V**	**1.512**	**1.509**	**1.515**	**1.519**	**1.513**
	V	***1.537***	***1.532***	***1.522***	***1.532***	***1.528***
C3-O10	**V**	**1.407**	**1.490**	**1.380**	**1.364**	**1.381**
	L1	***1.430***	***1.429***	***1.427***	***1.374***	***1.370***
O10-H22	H3	0.922	1.345	2.062	2.947	4.432
	H3	*0.960*	*1.191*	*1.439*	*2.279*	*3.963*
C3-H15	**V**	**1.100**	**1.145**	**1.140**	**1.143**	**1.154**
	IH	***1.090***	***1.117***	***1.139***	***1.121***	***1.144***
C4-C5	**L1**	**1.539**	**1.525**	**1.521**	**1.512**	**1.509**
	IL	***1.540***	***1.535***	***1.534***	***1.532***	***1.533***
C4-O11	**V**	**1.412**	**1.432**	**1.153**	**1.158**	**1.475**
	H1	***1.430***	***1.433***	***1.445***	***1.452***	***1.467***
O11-H23	V	0.982	0.932	1.005	0.932	0.972
	V	*0.960*	*0.938*	*0.995*	*0.927*	*0.960*
C4-H16	**V**	**1.101**	**1.137**	**1.121**	**1.141**	**1.135**
	IH	***1.090***	***1.111***	***1.130***	***1.117***	***1.138***
C5-C6	**IL**	**1.534**	**1.489**	**1.448**	**1.437**	**1.479**
	V	***1.540***	***1.516***	***1.439***	***1.477***	***1.529***
C6-O12	V	1.100	1.543	1.099	1.210	1.123
	V	*1.090*	*1.167*	*1.127*	*1.182*	*1.132*
O12-H24	V	0.975	1.013	0.988	1.033	1.000
	V	*0.960*	*1.021*	*1.031*	*1.080*	*1.081*
C6-H18	L2	1.418	1.404	1.380	1.346	1.339
	L2	*1.430*	*1.417*	*1.374*	*1.314*	*1.274*
C6-H19	H3	1.100	1.108	2.360	3.401	5.114
	H3	*1.090*	*1.201*	*1.659*	*2.450*	*4.717*
C5-H17	**V**	**1.100**	**1.227**	**1.222**	**1.260**	**1.235**
	V	***1.090***	***1.158***	***1.177***	***1.434***	***1.152***
C5-O7	**V**	**1.432**	**1.437**	**1.440**	**1.439**	**1.432**
	V	***1.433***	***1.434***	***1.437***	***1.434***	***1.429***
O7-C1	**V**	**1.431**	**1.420**	**1.419**	**1.428**	**1.430**
	V	***1.433***	***1.430***	***1.427***	***1.442***	***1.456***

[a]See Table 2 for notation.

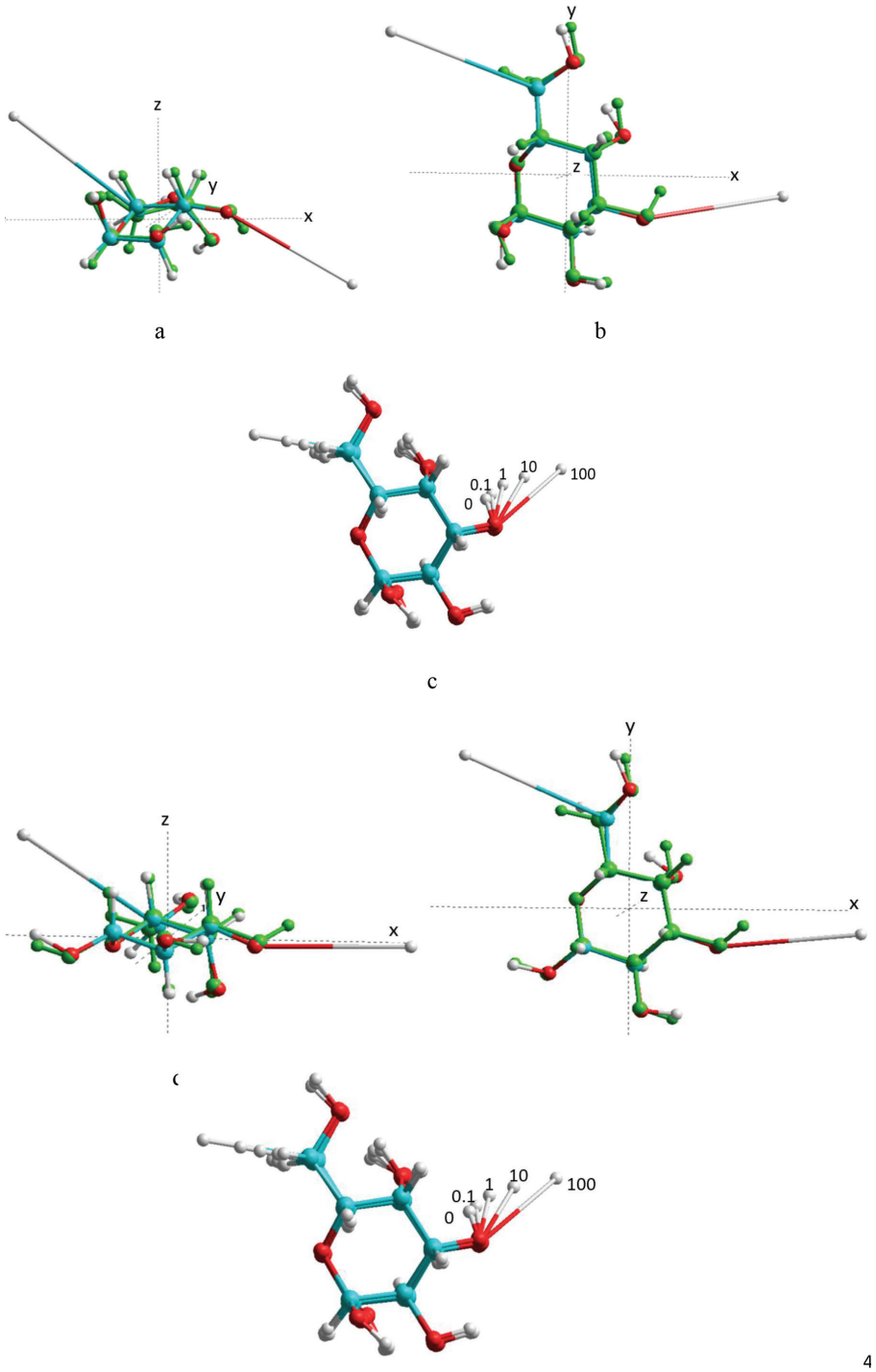

Figure 6. Simplified visualisation of the effect of SMF upon conformation and bond length of α-D- and β-D-galactose anomers (**a–c** and **d–f** respectively), situated in the Cartesian system. (see Fig. 2 for notation).

Table 7. Properties of the α- and β-D-fructopyranose and corresponding α- and β-D-fructofuranose molecules situated along the x-axis of the Cartesian system in SMF of the flux density of 0 to 100 AFU[a].

Property	Anomer	Flux density [AFU]				
		0	0.1	1	10	100
Dipole moment [D]	α-D-Fru*p*	3.63	3.67	3.76	3.93	4.24
	β-D-Fru*p*	3.60	3.61	3.69	3.86	4.16
	α-D-Fru*f*	3.68	3.69	3.87	3.92	4.16
	β-D-Fru*f*	3.66	3.71	3.85	3.90	4.09
Heat of formation [kcal/mole]	α-D-Fru*p*	-1193.2	-1190.4	-1153.8	-1140.6	-1096.5
	β-D-Fru*p*	-1205.5	-1203.2	-1199.9	-1156.7	-1026.5
	α-D-Fru*f*	-1255.6	-1253.5	-1231.5	-1231.5	-1201.8
	β-D-Fru*f*	-1245.6	-1243.5	-1238.6	-1221.4	-1198.5

[a]Upper and lower values (in italics) are for α- and β-isomers, respectively.

O7β, O8β, O9, O10 and H15α atoms. Small and irregular changes of electron density could be observed at C3, C4α, O11, H13, H14β, H15β and H16 atoms. Remarkable changes were noted at the C1, C5 and C2 atoms.

In fact, in a real molecule, all hydrogen atoms of the OH groups changed their positions by free rotation because of the practically identical energy between particular rotamers of those groups. This problem was well illustrated by the results of computation for the twin hydrogen H18 and H19 atoms. Due to accepted computation methodology, the free rotation around the C5-C6 bond was eliminated. In consequence, the H18 atom holds a considerable negative charge, whereas the H19 atom took increased positive charge density. As a result, results of the computations for particular rotamers could not be interpreted in detail in this case as well as in the cases of subsequently discussed carbohydrates. For D-glucose, these restrictions were also valid for the H20, H21, H22, H23, H24 and O12 atoms. Results of detailed analysis of the remaining O7, O8, O9, O10, O11, C1, C2, C3, C4, C5, C6, H13, H14, H15 and H16 atoms are identified in Table 2.

Generally, atoms of the pyranose skeleton were moderately sensitive to SMF, although increasing SMF flux density considerably decreased basicity of the ring O5 atom in the β-anomer. The O and H atoms were the most and least sensitive, respectively, to the effect of SMF. In the group bound to the C3 atom perpendicularly to the field, an increase in the flux density decreased the negative charge density at the O10 atom and the positive charge density at the H22 atom. It suggested a decrease in the acidity of that group. In the quasi-parallel orientated O8-H20 group, SMF evoked the opposite effect. Thus, the accepted orientation of the molecule under consideration appeared very essential. One of the biochemically most important OH group at the C6 atom turned more acidic and that effect could noticeably influence the biochemistry of D-glucose.

Review of Table 2 also identified that increased positive charge density at the C1 in the α-anomer favoured attacks of various Lewis bases at this position. Such reactions were also important from the biochemical point of view. Simultaneously, the reactivity of the β-anomer involving this position was partly inhibited as the positive

Table 8. Charge density [a.u] at particular atoms of the α- and β-D-glucose molecules depending on SMF flux density [AFU].

Atom	Flux density [AFU]					
	Tendency	0	0.1	1.0	10	100
C1	**H3**	**-0.049**	**-0.068**	**0.048**	**0.147**	**0.275**
	H3	***-0.027***	***-0.036***	***-0.018***	***0.131***	***0.493***
C2	**H2**	**0.118**	**0.159**	**0.166**	**0.169**	**0.173**
	L2	***0.103***	***0.098***	***0.098***	***0.062***	***-0.027***
C3	**V**	**0.098**	**0.051**	**0.052**	**0.050**	**0.052**
	V	***0.130***	***0.145***	***0.146***	***0.131***	***0.089***
C4	**IL**	**0.160**	**0.084**	**0.076**	**0.071**	**0.096**
	V	***0.175***	***0.185***	***0.144***	***0.117***	***0.179***
C5	**V**	**0.541**	**0.576**	**0.552**	**0.552**	**0.487**
	V	***0.522***	***0.547***	***0.550***	***0.525***	***0.481***
C6	**IL**	**0.015**	**-0.068**	**-0.044**	**-0.046**	**-0.002**
	H1	***-0.025***	***-0.021***	***0.015***	***0.027***	***0.032***
O7	**V**	**-0.578**	**-0.578**	**-0.570**	**-0.561**	**-0.540**
	V	***-0.598***	***-0.598***	***-0.607***	***-0.586***	***-0.568***
O8	**L**	**-0.699**	**-0.709**	**-0.733**	**-0.741**	**-0.758**
	IH	***-0.705***	***-0.701***	***-0.700***	***-0.691***	***-0.661***
O9	**H1**	**-0.751**	**-0.709**	**-0.688**	**-0.688**	**-0.683**
	H1	***-0.748***	***-0.743***	***-0.715***	***-0.693***	***-0.668***
O10	**V**	**-0.734**	**-0.463**	**-0.453**	**-0.472**	**-0.586**
	IH	***-0.752***	***-0.709***	***-0.563***	***-0.434***	***-0.572***
O11	**V**	**-0.676**	**-0.635**	**-0.631**	**-0.643**	**-0.639**
	V	***-0.728***	***-0.744***	***-0.751***	***-0.740***	***-0.754***
O12	H2	-0.691	-0.660	-0.662	-0.657	-0.540
	IL	*-0.694*	*-0.697*	*-0.690*	*-0.713*	*-0.725*
H13	**H2**	**0.180**	**0.210**	**0.245**	**0.260**	**0.289**
	V	***0.212***	***0.210***	***0.202***	***0.222***	***0.272***
H14	**L1**	**0.208**	**0.171**	**-0.048**	**-0.175**	**-0.260**
	IL	***0.192***	***0.194***	***0.188***	***-0.011***	***-0.329***
H15	**H1**	**0.171**	**0.178**	**0.196**	**0.201**	**0.206**
	IH	***0.169***	***0.161***	***0.162***	***0.184***	***0.212***
H16	**V**	**0.166**	**0.194**	**0.194**	**0.193**	**0.191**
	V	***0.176***	***0.172***	***0.171***	***0.185***	***0.187***
H17	**V**	**0.228**	**0.234**	**0.235**	**0.240**	**0.229**
	IH	***0.239***	***0.234***	***0.248***	***0.261***	***0.281***
H18	V	0.165	0.157	0.149	0.146	0.179
	V	*0.121*	*0.094*	*0.089*	*0.133*	*0.174*
H19	V	0.159	0.200	0.202	0.212	0.142
	V	*0.198*	*0.196*	*0.198*	*0.184*	*0.180*
H20	H2	0.360	0.422	0.434	0.446	0.467
	V	*0.413*	*0.413*	*0.408*	*0.414*	*0.424*
H21	V	0.386	0.413	0.411	0.423	0.420
	V	*0.415*	*0.421*	*0.415*	*0.417*	*0.428*
H22	V	0.418	0.116	0.099	0.110	0.130
	L2	*0.405*	*0.359*	*0.195*	*0.045*	*0.024*
H23	V	0.416	0.316	0.358	0.372	0.387
	V	*0.407*	*0.412*	*0.402*	*0.406*	*0.430*
H24	V	0.390	0.363	0.372	0.372	0.375
	H2	*0.198*	*0.408*	*0.411*	*0.418*	*0.427*

aSee Table 2 for notation.

Table 9. Bond lengths [Å] in the α- and β-D-fructopyranose molecules depending on the applied SMF flux density [AFU][a].

Bond	Flux density [AFU]					
	Tendency	0	0.1	1	10	100
C1-C2	**V**	**1.540**	**1.575**	**1.561**	**1.563**	**1.571**
	V	***1.540***	***1.537***	***1.545***	***1.530***	***1.516***
C1-H13	**H3**	**1.090**	**1.562**	**2.053**	**2.481**	**3.678**
	H3	***1.090***	***1.240***	***1.323***	***1.936***	***3.435***
C1-H14	**V**	**1.090**	**1.091**	**1.145**	**1.006**	**1.172**
	V	***1.090***	***1.102***	***1.116***	***1.126***	***1.100***
C2-C3	**V**	**1.537**	**1.559**	**1.544**	**1.568**	**1.519**
	V	***1.537***	***1.531***	***1.546***	***1.544***	***1.541***
C2-O8	**H1**	**1.430**	**1.433**	**1.437**	**1.437**	**1.439**
	H1	***1.430***	***1.435***	***1.435***	***1.445***	***1.473***
O8-H20	V	0.960	1.026	0.968	1.026	1.017
	V	*0.960*	*0.952*	*1.050*	*0.985*	*1.030*
C2-H15	**V**	**1.090**	**1.252**	**1.190**	**1.217**	**1.234**
	V	***1.090***	***1.217***	***1.178***	***1.215***	***1.198***
C3-C4	**V**	**1.537**	**1.562**	**1.570**	**1.568**	**1.566**
	IH	***1.537***	***1.546***	***1.564***	***1.571***	***1.524***
C3-O10	**V**	**1.430**	**1.470**	**1.415**	**1.394**	**1.389**
	IL	***1.430***	***1.396***	***1.370***	***1.371***	***1.368***
O10-H21	V	0.960	0.986	0.916	1.017	0.907
	V	*0.960*	*0.971*	*0.929*	*0.954*	*0.993*
C3-H16	**V**	**1.090**	**1.193**	**1.137**	**1.202**	**1.173**
	V	***1.090***	***1.127***	***1.113***	***1.122***	***1.1103***
C4-C5	**H1**	**1.540**	**1.621**	**1.622**	**1.627**	**1.628**
	H1	***1.540***	***1.547***	***1.560***	***1.575***	***1.598***
C4-O11	**V**	**1.430**	**1.547**	**1.527**	**1.522**	**1.517**
	V	***1.430***	***1.447***	***1.446***	***1.427***	***1.444***
O11-H22	H3	0.960	2.268	2.928	3.341	3.781
	H3	*0.960*	*1.333*	*1.972*	*2.847*	*4.491*
C4-H17	**V**	**1.090**	**1.137**	**1.110**	**1.137**	**1.116**
	V	***1.090***	***1.099***	***1.410***	***1.087***	***1.083***
C5-C6	**V**	**1.540**	**1.638**	**1.596**	**1.580**	**1.526**
	IH	***1.540***	***1.516***	***1.560***	***1.567***	***1.570***
C5-O9	**IL**	**1.430**	**1.374**	**1.364**	**1.354**	**1.356**
	V	***1.090***	***1.430***	***1.458***	***1.456***	***1.445***
O9-H23	V	0.960	1.035	0.910	1.016	0.897
	V	*0.960*	*1.013*	*0.913*	*0.982*	*1.022*
C6-O12	V	1.430	1.556	1.471	1.435	1.423
	IL	*1.430*	*1.413*	*1.378*	*1.388*	*1.375*
O12-H24	V	0.960	0.963	0.932	0.974	0.928
	V	*0.960*	*0.906*	*0.988*	*0.967*	*0.912*
C6-H18	V	0.960	1.101	1.119	1.080	1.111
	IL	*1.960*	*1.134*	*1.083*	*1.163*	*1.167*
C6-H19	H2	1.090	1.128	1.154	1.157	1.569
	V	*1.090*	*1.184*	*1.205*	*1.107*	*1.170*
C5-O7	**V**	**1.433**	**1.387**	**1.397**	**1.393**	**1.416**
	V	***1.432***	***1.417***	***1.392***	***1.402***	***1.400***
O7-C1	**IH**	**1.433**	**1.467**	**1.477**	**1.485**	**1.462**
	V	***1.433***	***1.454***	***1.481***	***1.470***	***1.470***

[a]See Table 2 for notation.

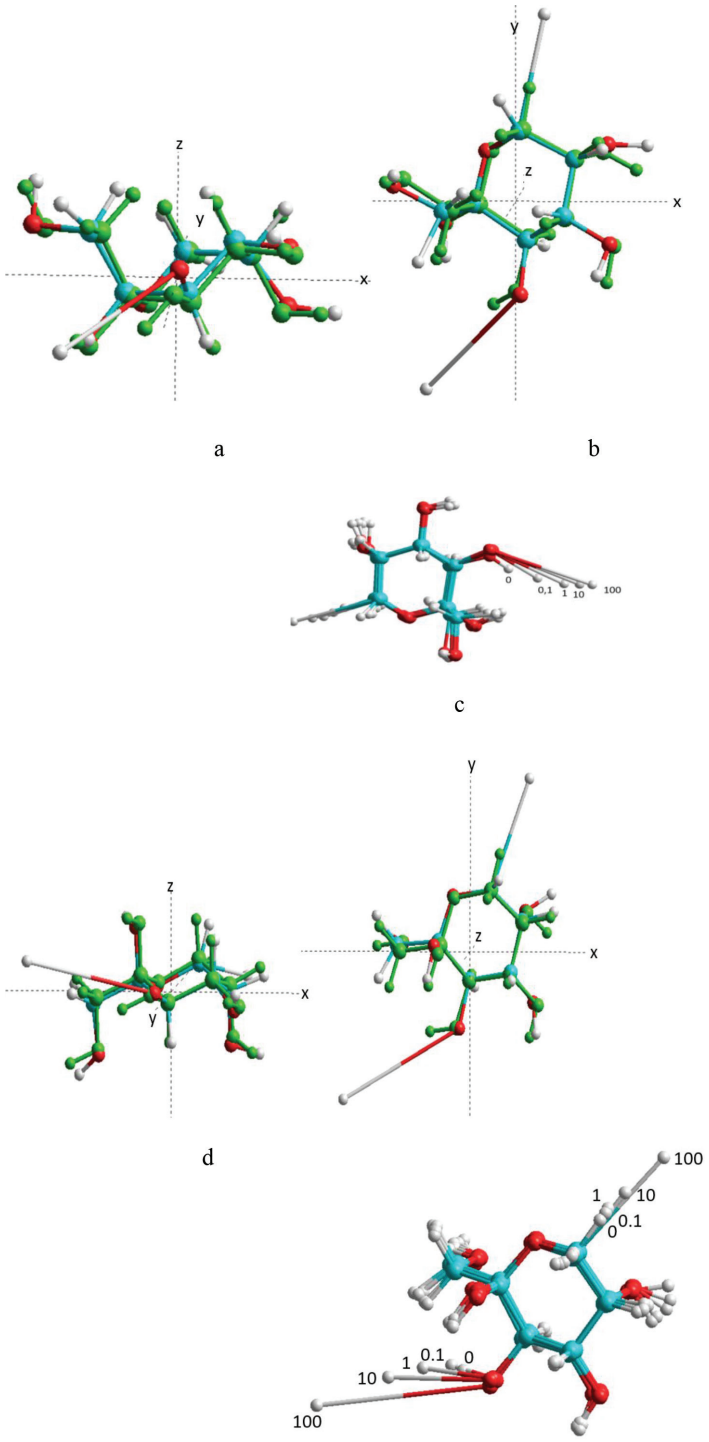

Figure 7. Simplified visualisation of the effect of SMF upon conformation and bond length of α-D- and β-D-fructopyranose anomers (**a–c** and **d–f** respectively), situated in the Cartesian system (see Fig. 2 for notation).

Table 10. Charge density [a.u] at particular atoms of the α- and β-D-glucose molecules depending on SMF flux density [AFU].

Atom		Flux density [AFU]				
	Tendency	0	0.1	1.0	10	100
C1	**IL**	**0.521**	**0.528**	**0.523**	**0.499**	**0.464**
	H2	***0.508***	***0.561***	***0.581***	***0.617***	***0.714***
C2	**L2**	**0.020**	**0.002**	**-0.012**	**-0.022**	**-0.037**
	IL	***0.155***	***0.118***	***0.080***	***0.058***	***0.059***
C3	**V**	**0.129**	**0.129**	**0.124**	**0.121**	**0.189**
	IL	***0.116***	***0.104***	***0.111***	***0.086***	***-0.005***
C4	**H1**	**0.115**	**0.122**	**0.128**	**0.130**	**0.140**
	L1	***0.092***	***0.080***	***0.079***	***0.071***	***0.032***
C5	**IH**	**0.097**	**0.086**	**0.109**	**0.206**	**0.405**
	L2	***0.034***	***0.015***	***-0.002***	***-0.023***	***-0.143***
C6	**IL**	**0.035**	**0.035**	**0.027**	**-0.016**	**-0.063**
	IL	***-0.006***	***-0.019***	***-0.038***	***-0.023***	***-0.038***
O7	**V**	**-0.589**	**-0.597**	**-0.604**	**-0.511**	**-0.620**
	V	***-0.625***	***-0.634***	***-0.676***	***-0.658***	***-0.642***
O8	**H1**	**-0.656**	**-0.639**	**-0.628**	**-0.625**	**-0.560**
	V	***-0.711***	***-0.718***	***-0.665***	***-0.686***	***-0.469***
O9	**IL**	**-0.712**	**-0.696**	**-0.670**	**-0.641**	**-0.680**
	H2	***-0.741***	***-0.714***	***-0.686***	***-0.588***	***-0.380***
O10	**IH**	**-0.711**	**-0.691**	**-0.677**	**-0.670**	**-0.680**
	IH	***-0.734***	***-0.712***	***-0.714***	***-0.699***	***-0.667***
O11	H1	-0.674	-0.641	-0.620	-0.605	-0.580
	H1	*-0.700*	*-0.702*	*-0.690*	*-0.675*	*-0.607*
O12	H2	-0.696	-0.682	-0.644	-0.500	-0.359
	IH	*-0.743*	*-0.724*	*-0.709*	*-0.722*	*-0.699*
H13	**H1**	**0.217**	**0.219**	**0.222**	**0.228**	**0.245**
	IL	***0.235***	***0.228***	***0.205***	***0.221***	***-0.218***
H14	**H1**	**0.180**	**0.182**	**0.184**	**0.188**	**0.189**
	IH	***0.184***	***0.182***	***0.192***	***0.198***	***0.259***
H15	**H1**	**0.205**	**0.205**	**0.207**	**0.212**	**0.225**
	V	***0.196***	***0.202***	***0.187***	***0.200***	***0.202***
H16	H1	0.167	0.170	0.178	0.196	0.244
	V	*0.173*	*0.164*	*0.139*	*0.076*	*0.190*
H17	L2	0.104	0.064	-0.004	-0.148	-0.470
	H1	*0.182*	*0.183*	*0.196*	*0.200*	*0.212*
H18	VI	0.169	0.161	0.159	0.175	0.248
	H	*0.173*	*0.176*	*0.202*	*0.194*	*0.217*
H19	V	0.148	0.142	0.143	0.154	0.171
	V	*0.173*	*0.159*	*0.174*	*0.162*	*0.179*
H20	V	0.365	0.364	0.366	0.374	0.388
	V	*0.415*	*0.433*	*0.451*	*0.408*	*0.124*
H21	H2	0.389	0.395	0.402	0.419	0.454
	V	*0.397*	*0.405*	*0.396*	*0.416*	*0.419*
H22	L2	0.387	0.373	0.355	0.341	0.295
	L2	*0.401*	*0.394*	*0.385*	*0.304*	*0.244*
H23	V	0.403	0.400	0.397	0.398	0.407
	V	*0.414*	*0.410*	*0.398*	*0.397*	*0.401*
H24	L3	0.388	0.373	0.335	0.198	0.005
	V	*0.412*	*0.411*	*0.404*	*0.410*	*0.416*

[a]See Table 2 for notation.

Table 11. Bond lengths [Á] in the α- and β-D-fructofuranose molecules depending on the applied SMF flux density [AFU][a].

Bond		Flux density [AFU]				
	tendency	0	0.1	1	10	100
C1-C2	**H1**	**1.540**	**1.549**	**1.559**	**1.570**	**1.592**
	H3	***1.539***	***1.624***	***1.847***	***2.084***	***2.422***
C1-O8	**V**	**1.413**	**1.408**	**1.406**	**1.406**	**1.409**
	V	***1.430***	***1.365***	***1.273***	***1.304***	***1.225***
O8-H20	H1	0.960	0.955	0.970	0.978	0.985
	H3	*0.960*	*0.994*	*1.155*	*1.183*	*1.783*
C1-C5	**L1**	**1.535**	**1.521**	**1.511**	**1.502**	**1.495**
	IL	***1.540***	***1.527***	***1.509***	***1.473***	***1.485***
C5-O11	IH	1.412	1.389	1.586	1.376	1.848
	V	*1.430*	*1.439*	*1.442*	*1.421*	*1.370*
O11-H21	V	0.960	0.960	0.970	0.978	0.995
	V	*0.960*	*0.992*	*0.982*	*0.961*	*1.001*
C5-H16	V	1.091	1.151	1.150	1.121	1.112
	V	*1.090*	*1.145*	*1.132*	*1.128*	*1.132*
C5-H17	H3	1.091	1.365	1.586	1.936	2.922
	V	*1.090*	*1.337*	*1.242*	*1.358*	*1.255*
C2-C3	**V**	**1.523**	**1.514**	**1.513**	**1.519**	**1.541**
	IL	***1.539***	***1.536***	***1.497***	***1.477***	***1.522***
C2-O9	**V**	**1.412**	**1.422**	**1.427**	**1.426**	**1.395**
	V	***1.430***	***1.398***	***1.327***	***1.298***	***1.177***
O9-H22	H3	0.959	1.173	1.322	1.487	2.036
	H3	*0.960*	*1.063*	*1.069*	*1.322*	*3.213*
C2-H13	H1	1.092	1.109	1.120	1.124	1.153
	V	*1.090*	*1.172*	*1.142*	*1.131*	*1.153*
C3-C4	**IL**	**1.524**	**1.517**	**1.514**	**1.511**	**1.515**
	H1	***1.540***	***1.544***	***1.596***	***1.601***	***1.610***
C3-O10	**IL**	**1.412**	**1.398**	**1.390**	**1.386**	**1.399**
	H2	***1.430***	***1.945***	***1.533***	***1.577***	***1.614***
O10-H23	V	0.960	1.000	1.000	0.983	0.946
	V	*0.960*	*0.971*	*0.986*	*1.001*	*0.995*
C3-H14	**H1**	**1.091**	**1.103**	**1.131**	**1.146**	**1.178**
	V	***1.090***	***1.453***	***1.119***	***1.132***	***1.106***
C4-O7	**H1**	**1.414**	**1.416**	**1.425**	**1.441**	**1.465**
	V	***1.431***	***1.421***	***1.420***	***1.420***	***1.432***
C4-C6	**IH**	**1.531**	**1.532**	**1.536**	**1.540**	**1.5397**
	V	***1.540***	***1.558***	***1.539***	***1.561***	***1.557***
C4-H15	**H1**	**1.092**	**1.142**	**1.166**	**1.172**	**1.198**
	V	***1.090***	***1.207***	***1.079***	***1.069***	***1.036***
C6-O12	IL	1.411	1.417	1.410	1.391	1.360
	V	*1.430*	*1.450*	*1.580*	*1.499*	*1.505*
O12-H24	H3	0.960	1.166	1.378	1.902	3.080
	V	*0.960*	*0.990*	*0.961*	*0.927*	*0.958*
C6-H18	V	1.090	1.134	1.132	1.122	1.122
	V	*1.090*	*1.273*	*1.143*	*1.233*	*1.201*
C6-H19	H2	1.098	1.190	1.246	1.257	1.290
	IH	*1.090*	*1.139*	*1.147*	*1.139*	*1.155*
O7-C1	**L1**	**1.421**	**1.420**	**1.420**	**1.417**	**1.409**
	V1	***1.431***	***1.457***	***1.437***	***1.402***	***1.412***

[a]See Table 2 for notation.

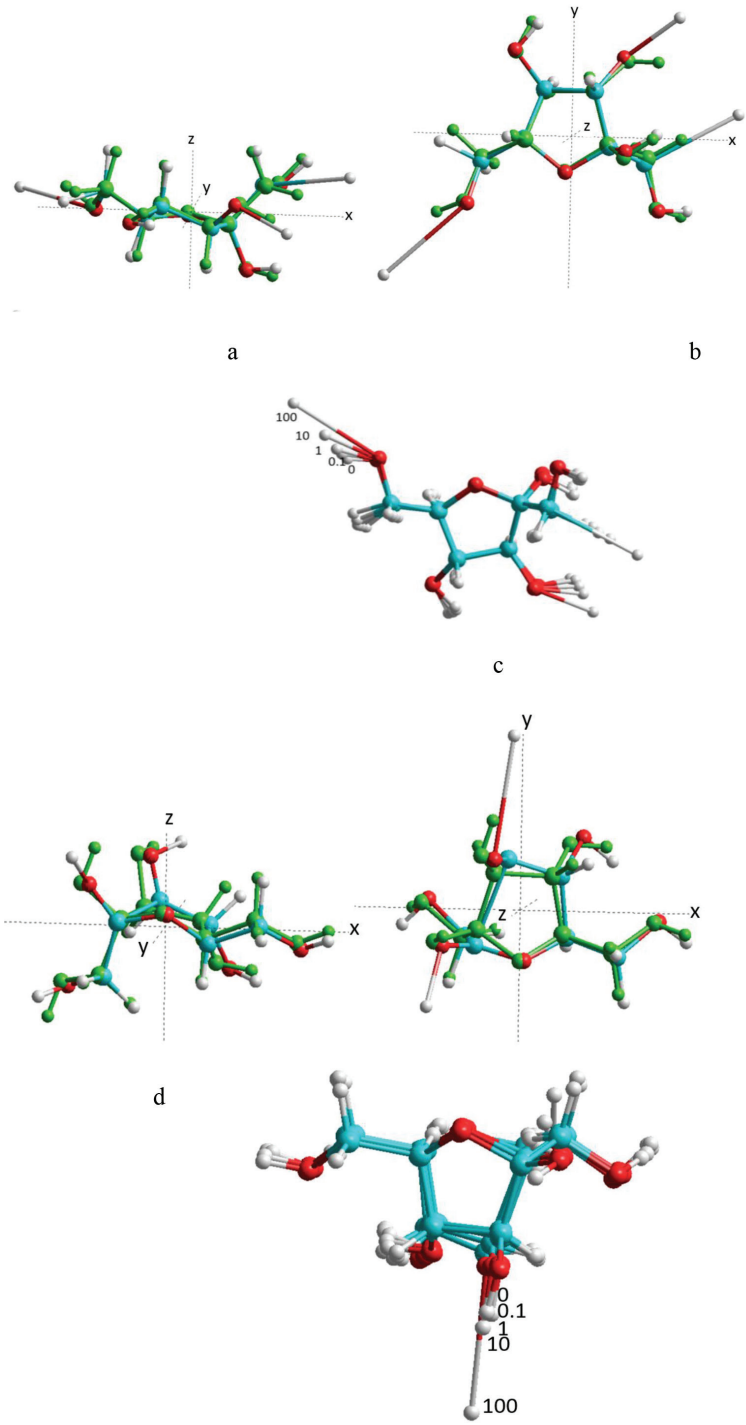

Figure 8. Simplified visualisation of the effect of SMF upon conformation and bond length of α-D- and β-D-fructofuranose anomers (**a–c** and **d–f** respectively), situated in the Cartesian system (see Fig. 2 for notation).

Table 12. Properties of the α- and β-D-xylose molecules situated along the x-axis of the Cartesian system in SMF of the flux density of 0 to 100 AFU[a].

Property	Anomer	Flux density [AFU]				
		0	0.1	1	10	100
Dipole moment [D]	α-D-Xyl*p*	4.22	4.24	4.31	4.67	4.73
	β-D-Xyl*p*	1.22	1.23	1.29	1.37	1.47
	α-D-Xyl*f*	4.85	4.89	4.94.	5.15	5.69
	β-D-Xyl*f*	4.87	4.89	4.95	5.01	5.19
Heat of formation [kcal/mole]	α-D-Xyl*p*	-1143.2	-1127.4	-1089.6	-1061.2	-1005.4
	β-D-Xyl*p*	-1154.2	1147.3	-1110.3	-1089.5	-1021.8
	α-D-Xyl*f*	-1076.2	—1075.4	-1069.4	-1041.3	-995.6
	β-D-Xyl*f*	-1051.2	-1049.5	-1036.4	-1004.4	-952.3

[a]Upper and lower values (in italics) are for α- and β-isomers, respectively.

charge density at this atom declined under the influence of SMF. The SMF induced an increase in the positive charge density at the C6 atom. It was non-beneficial for enzymatic processes starting from esterification with adenosine-triphosphate (ATP) at C6-O24 and the functioning of the Entner-Doudorff metabolic pathway (Conway 1992).

An insight into the effect of SMF upon the length of bonds in the molecules of both anomers (Table 3) suggested that these changes resulted from a deformation of the molecules and their deviation from the initially-established location of the molecules along the x-axis. Tendencies of the changes of computed values with an increase in the flux density (Table 3) pointed to a uniform increase in the length of the valence bonds, that is, to weakening their energy. Simultaneously, strongly polarised bonds, with participation of the C1 atom, were regularly shortened, whereas the length of the C3-C4, C3-O10, C3-C5 and C5-O7 bonds varied irregularly. Generally, in the 28 analysed bonds in each anomer, 16 bonds were elongated, four bonds were shortened and the length of eight bonds varied irregularly against increased SMF flux density. These results supported the hypothesis on the weakening of the bonding electron pair. The SMF generated shortening of the C1-O8 bond and elongation of the O8-H20 bond seemed to be the most important. This effect implied the increased susceptibility of the hemi-acetal ring to its opening. Hence, SMF should favour a shift of the mutarotation equilibrium towards the open chain form of D-glucose. This fact could promote the Maillard reaction which proceeds on the open chain forms of saccharides (Grandhee and Monnier 1991).

Visualisation of the data from Table 3 (Fig. 5) also includes non-analysable bonds. The conformation of particular anomers is presented in the form of superposition of the molecules without SMF (green colour) and molecules in the SMF of 100 AFU (blue colour). The oxygen atoms are marked red. Structures *a* and *d* are given as the projection along the *y*-axis, whereas the *b* and *e* structures are projections along the *z*-axis. Structures *c* and *f* are superpositions of the same molecules demonstrating the SMF flux density-dependent change in the bond lengths in the molecules under consideration. Structures in Fig. 5 demonstrate a small effect of SMF upon the conformation of both anomers and a significant effect upon the bond lengths of some peripheral

Table 13. Charge density [a.u] at particular atoms of the α- and β-D-glucose molecules depending on SMF flux density [AFU].

Atom		Flux density [AFU]				
	Tendency	0	0.1	1.0	10	100
C1	**H2**	**0.388**	**0.400**	**0.424**	**0.450**	**0.460**
	V	***0.474***	***0.476***	***0.460***	***0.478***	***0.492***
C2	**L2**	**0.093**	**0.085**	**0.035**	**-0.039**	**-0.059**
	L2	***0.087***	***0.058***	***0.057***	***-0.032***	***-0.055***
C3	**V**	**0.191**	**0.191**	**0.130**	**0.142**	**0.134**
	V	***0.119***	***0.117***	***0.108***	***0.110***	***0.109***
C4	**IH**	**0.142**	**0.145**	**0.161**	**0.172**	**0.167**
	IH	***0.163***	***0.179***	***0.195***	***0.215***	***0.196***
C5	**H2**	**-0.042**	**-0.038**	**-0.029**	**0.010**	**0.125**
	H2	***-0.059***	***-0.048***	***-0.058***	***-0.040***	***0.066***
O6	**V**	**-0.602**	**-0.603**	**-0.568**	**-0.560**	**-0.605**
	V	***-0.590***	***-0.590***	***-0.585***	***-0.569***	***-0.577***
O7	**V**	**-0.695**	**-0.697**	**-0.749**	**-0.682**	**-0.704**
	V	***-0.683***	***-0.665***	***-0.661***	***-0.653***	***-0.674***
O8	**H2**	**-0.735**	**-0.730**	**-0.649**	**-0.522**	**-0.508**
	H2	***-0.726***	***-0.703***	***-0.684***	***-0.494***	***-0.485***
O9	**H1**	**-0.751**	**-0.745**	**-0.719**	**-0.717**	**-0.714**
	H1	***-0.743***	***-0.727***	***-0.721***	***-0.706***	***-0.706***
O10	**V**	**-0.728**	**-0.726**	**-0.725**	**-0.748**	**-0.768**
	V	***-0.730***	***-0.729***	***-0.731***	***-0.748***	***-0.765***
H11	**IH**	**0.160**	**0.161**	**0.166**	**0.193**	**0.190**
	V	***0.160***	***0.160***	***0.156***	***0.166***	***0.172***
H12	**V**	**0.188**	**0.187**	**0.185**	**0.200**	**0.200**
	V	***0.197***	***0.196***	***0.195***	***0.201***	***0.202***
H13	**V**	**0.191**	**0.191**	**0.194**	**0.206**	**0.201**
	V	***0.176***	***0.175***	***0.173***	***0.186***	***0.190***
H14	**V**	**0.169**	**0.164**	**0.161**	**0.182**	**0.205**
	V	***0.180***	***0.173***	***0.176***	***0.183***	***0.196***
H15	**V**	**0.228**	**0.224**	**0.234**	**0.071**	**0.258**
	V	***0.208***	***0.206***	***0.208***	***0.194***	***0.239***
H16	**V**	**0.194**	**0.193**	**0.201**	**0.188**	**-0.062**
	V	***0.181***	***0.168***	***0.177***	***0.105***	***-0.037***
H17	V	0.410	0.405	0.373	0.386	0.396
	V	*0.367*	*0.355*	*0.345*	*0.353*	*0.369*
H18	IL	0.398	0.392	0.335	0.238	0.230
	L1	*0.383*	*0.366*	*0.353*	*0.203*	*0.202*
H19	V	0.415	0.415	0.413	0.407	0.412
	V	*0.419*	*0.416*	*0.414*	*0.411*	*0.413*
H 20	IH	0.414	0.414	0.426	0.423	0.443
	IH	*0.417*	*0.415*	*0.420*	*0.435*	*0.445*

[a]See Table 2 for notation.

C-H bonds. They are the C6-H19 and O10-H22 bonds. An increasing flux density generated a considerable negative charge density at the H18 atom. It made the O12-H24 bond relatively slightly polarised, that is, capable of interaction of electrons of that bond with SMF.

Table 14. Bond lengths [Á] in the α- and β-D-xylopyranose molecules depending on the applied SMF flux density [AFU][a].

Bond		Flux density [AFU]				
	Tendency	0	0.1	1	10	100
C1-C2	**V**	**1.540**	**1.559**	**1.553**	**1.538**	**1.573**
	V	***1.540***	***1.555***	***1.535***	***1.567***	***1.562***
C1-O7	**V**	**1.430**	**1.476**	**1.603**	**1.523**	**1.497**
	V	***1.430***	***1.433***	***1.430***	***1.409***	***1.416***
O7-H17	V	0.960	0.965	0.952	0.956	0.953
	V	*0.960*	*0.971*	*0.968*	*0.964*	*0.951*
C1-H11	**V**	**1.090**	**1.119**	**1.149**	**1.097**	**1.124**
	V	***1.090***	***1.146***	***1.160***	***1.149***	***1.153***
C2-O8	**V**	**1.430**	**1.500**	**1.516**	**1.388**	**1.425**
	V	***1.430***	***1.504***	***1.523***	***1.403***	***1.431***
O8-H18	H3	0.960	1.226	1.565	2.366	3.116
	H3	*0.960*	*1.220*	*1.358*	*2.532*	*3.116*
C2-H12	**V**	**1.090**	**1.128**	**1.159**	**1.124**	**1.139**
	H1	***1.090***	***1.128***	***1.135***	***1.135***	***1.136***
C2-C3	**IH**	**1.538**	**1.542**	**1.580**	**1.511**	**1.584**
	IH	***1.537***	***1.567***	***1.583***	***1.602***	***1.597***
C3-O9	**V**	**1.430**	**1.404**	**1.379**	**1.407**	**1.393**
	V	***1.430***	***1.398***	***1.394***	***1.397***	***1.393***
O9-H19	V	0.960	0.957	0.952	0.953	0.953
	V	*0.960*	*0.958*	*0.958*	*0.958*	*0.952*
C3-H13	**V**	**1.090**	**1.127**	**1.152**	**1.125**	**1.145**
	V	***1.090***	***1.132***	***1.135***	***1.144***	***1.140***
C3-C4	**V**	**1.537**	**1.609**	**1.652**	**1.622**	**1.630**
	V	***1.537***	***1.614***	***1.640***	***1.603***	***1.624***
C4-O10	V	1.430	1.408	1.367	1.412	1.373
	L1	*1.430*	*1.418*	*1.392*	*1.380*	*1.366*
O10-H20	H1	0.960	0.973	0.988	0.989	1.002
	H1	*0.960*	*0.977*	*0.978*	*0.997*	*1.002*
C4-H14	**H2**	**1.090**	**1.166**	**1.240**	**1.270**	**1.293**
	H2	***1.090***	***1.169***	***1.189***	***1.295***	***1.309***
C4-C5	**V**	**1.540**	**1.553**	**1.555**	**1.498**	**1.519**
	V	***1.540***	***1.563***	***1.568***	***1.492***	***1.513***
C5-H15	**H2**	**1.090**	**1.184**	**1.283**	**1.589**	**1.878**
	H2	***1.090***	***1.188***	***1.221***	***1.637***	***1.897***
C5-H16	**V**	**1.090**	**1.110**	**1.108**	**1.180**	**1.085**
	V	***1.090***	***1.118***	***1.115***	***1.162***	***1.104***
C5-O6	**V**	**1.432**	**1.559**	**1.482**	**1.233**	**1.394**
	V	***1.432***	***1.372***	***1.446***	***1.371***	***1.390***
C1-O6	**V**	**1.432**	**1.385**	**1.233**	**1.439**	**1.369**
	V	***1.432***	***1.414***	***1.392***	***1.419***	***1.403***

[a]See Table 2 for notation.

D-Galactose

This aldohexose resides in two anomeric pyranose forms (Fig. 2) interconverting through an open-chain thermodynamically unstable structure. α-D-Galactopyranose (α-D-Gal*p*) can be found in oligo- and polysaccharides, plant mucous and gums and plant glycosides (Maton et al. 1993; Tomasik 1997; Campbell et al. 2006; Tomasik

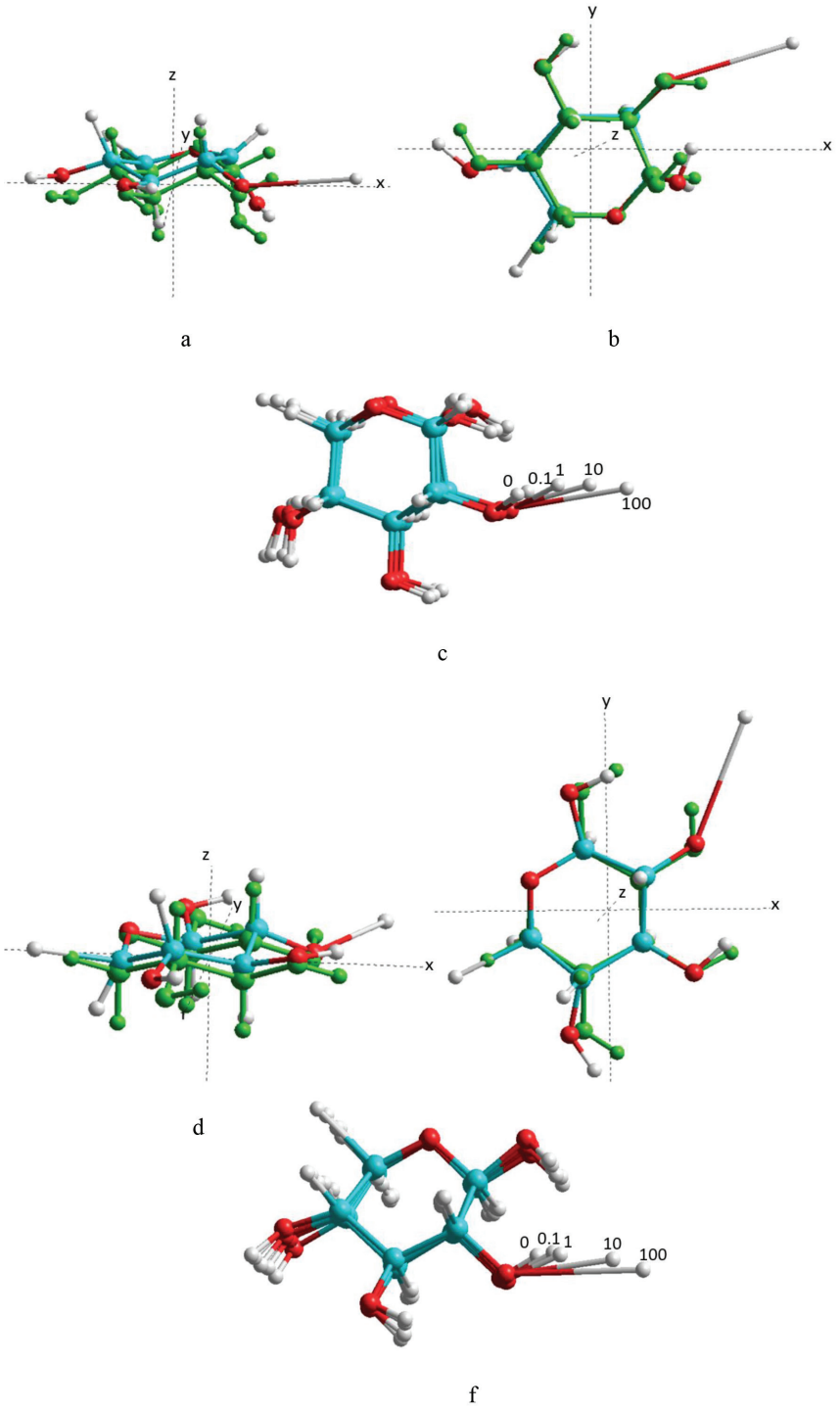

Figure 9. Simplified visualisation of the effect of SMF upon conformation and bond length of α-D- and β-D-xylopyranose anomers (**a–c** and **d–f** respectively) situated in the Cartesian system (see Fig. 2 for notation).

Table 15. Charge density [a.u] at particular atoms of the α- and β-D-glucose molecules depending on SMF flux density [AFU].

Atom		Flux density [AFU]				
	Tendency	0	0.1	1.0	10	100
C1	**V**	**0.350**	**0.348**	**0.353**	**0.353**	**0.343**
	V	***0.433***	***0.431***	***0.441***	***0.451***	***0.451***
C2	**H1**	**0.171**	**0.171**	**0.180**	**0.187**	**0.207**
	V	***0.093***	***0.092***	***0.080***	***0.095***	***0.068***
C3	**IL**	**0.080**	**0.046**	**0.029**	**0.018**	**0.022**
	V	***0.111***	***0.098***	***0.073***	***0.089***	***0.077***
C4	**V**	**0.152**	**0.178**	**0.158**	**0.115**	**0.029**
	L2	***0.123***	***0.181***	***0.153***	***0.097***	***0.007***
C5	**H2**	**-0.018**	**-0.010**	**0.084**	**0.219**	**0.409**
	IH	***-0.044***	***-0.046***	***-0.026***	***0.092***	***0.342***
O6	**V**	**-0.622**	**-0.627**	**-0.627**	**-0.618**	**-0.591**
	V	***-0.606***	***-0.609***	***-0.615***	***-0.600***	***-0.560***
O7	**H1**	**-0.680**	**-0.670**	**-0.670**	**-0.669**	**-0.669**
	IH	***-0.675***	***-0.673***	***-0.661***	***-0.647***	***-0.649***
O8	**IH**	**-0.694**	**-0.671**	**-0.670**	**-0.665**	**-0.670**
	IH	***-0.705***	***-0.699***	***-0.668***	***-0.687***	***-0.634***
O9	**H2**	**-0.743**	**-0.721**	**-0.698**	**-0.675**	**-0.568**
	H2	***-0.735***	***-0.729***	***-0.709***	***-0.681***	***-0.652***
O10	H2	-0.742	-0.733	-0.717	-0.695	-0.527
	H1	*-0.736*	*-0.735*	*-0.726*	*-0.700*	*-0.661*
H11	**H2**	**0.183**	**0.182**	**0.184**	**0.187**	**0.201**
	V	***0.201***	***0.200***	***0.195***	***0.192***	***0.199***
H12	**L1**	**0.193**	**0.185**	**0.176**	**0.176**	**0.170**
	V	***0.192***	***0.191***	***0.172***	***0.150***	***0.164***
H13	**IH**	**0.199**	**0.191**	**0.195**	**0.205**	**0.219**
	V	***0.187***	***0.185***	***0.184***	***0.195***	***0.205***
H14	**IH**	**0.193**	**0.190**	**0.198**	**0.205**	**0.238**
	V	***0.180***	***0.181***	***0.178***	***0.185***	***0.214***
H15	H2	0.177	0.170	0.179	0.190	0.237
	V	*0.183*	*0.181*	*0.176*	*0.205*	*0.227*
H16	L3	0.172	0.145	0.021	-0.145	-0.506
	L3	*0.181*	*0.178*	*0.140*	*-0.037*	*-0.369*
H17	V	0.399	0.396	0.397	0.398	0.411
	V	*0.387*	*0.388*	*0.387*	*0.376*	*0.384*
H18	V	0.397	0.387	0.393	0.391	0.399
	V	*0.398*	*0.396*	*0.385*	*0.398*	*0.356*
H19	L2	0.423	0.427	0.414	0.396	0.291
	V	*0.418*	*0.420*	*0.422*	*0.399*	*0.393*
H20	H1	0.412	0.415	0.421	0.429	0.456
	H1	*0.400*	*0.413*	*0.419*	*0.428*	*0.439*

[a]See Table 2 for notation.

2007a; Tomasik 2007b; Heldt and Piechulla 2010; Keung and Mehta 2015; Churuangsuk et al. 2018; Reynolds et al. 2019). Jointly with α-D-glucose, it constitutes lactose, known as milk sugar. In fauna organisms, it is hydrolytically liberated from lactose. In these organisms, it is converted into galactoso-6-phosphate involving ATP α-D-galactose. The latter reacts with galactoso-1-phosphate uridinyltransferase into UDP-galactose which is subsequently transformed with UDP-galactoso-4-epimerase

Table 16. Bond lengths [Å] in the α- and β-D-xylofuranose molecules depending on the applied SMF flux density [AFU][a].

Bond	Flux density [AFU]					
	Tendency	0	0.1	1	10	100
C1-C2	**H1**	**1.525**	**1.555**	**1.593**	**1.619**	**1.666**
	H1	***1.528***	***1.534***	***1.562***	***1.603***	***1.606***
C1-O7	**L1**	**1.420**	**1.404**	**1.398**	**1.391**	**1.374**
	V	***1.411***	***1.404***	***1.395***	***1.429***	***1.424***
O7-H17	V	0.960	1.037	0.966	1.031	0.972
	V	*0.960*	*0.954*	*0.979*	*1.010*	*0.975*
C1-H11	**V**	**1.090**	**1.143**	**1.123**	**1.143**	**1.178**
	V	***1.091***	***1.103***	***1.137***	***1.106***	***1.124***
C2-C3	**V**	**1.528**	**1.530**	**1.530**	**1.536**	**1.555**
	V	***1.532***	***1.531***	***1.536***	***1.548***	***1.599***
C2-O8	**L1**	**1.412**	**1.382**	**1.342**	**1.323**	**1.292**
	IL	***1.412***	***1.408***	***1.369***	***1.319***	***1.330***
O8-H18	V	0.960	1.101	1.080	1.185	1.187
	IH	*0.960*	*0.981*	*1.142*	*1.111*	*1.341*
C2-H12	**V**	**1.091**	**1.110**	**1.126**	**1.113**	**1.179**
	V	***1.091***	***1.082***	***1.153***	***1.166***	***1.128***
C3-C4	**V**	**1.540**	**1.568**	**1.567**	**1.569**	**1.558**
	H1	***1.537***	***1.542***	***1.581***	***1.676***	***1.659***
C3-O9	**V**	**1.413**	**1.372**	**1.370**	**1.375**	**1.391**
	V	***1.413***	***1.405***	***1.359***	***1.397***	***1.307***
O9-H19	H2	0.960	1.053	1.171	1.246	1.579
	IH	*0.960*	*0.981*	*1.047*	*1.321*	*1.267*
C3-H13	**V**	**1.091**	**1.222**	**1.225**	**1.200**	**1.121**
	V	***1.091***	***1.111***	***1.231***	***1.100***	***1.231***
C4-C5	**IL**	**1.533**	**1.494**	**1.463**	**1.448**	**1.461**
	IL	***1.533***	***1.523***	***1.475***	***1.434***	***1.449***
C5-O10	IL	1.411	1.401	1.401	1.385	1.339
	V	*1.412*	*1.410*	*1.221*	*1.336*	*1.355*
O10-H20	V	0.960	0.953	0.967	0.957	1.004
	V	*0.960*	*0.948*	*1.189*	*1.017*	*0.984*
C5-H15	H3	1.090	1.284	1.681	2.068	3.362
	H3	*1.098*	*1.418*	*1.390*	*1.708*	*2.636*
C5-H16	V	1.091	1.154	1.112	1.123	1.088
	V	*1.092*	*1.121*	*1.151*	*1.096*	*1.108*
C4-H14	**H2**	**1.091**	**1.115**	**1.119**	**1.123**	**1.153**
	V	***1.092***	***1.085***	***1.142***	***1.142***	***1.128***
C4-O6	**H1**	**1.417**	**1.438**	**1.464**	**1.469**	**1.472**
	H1	***1.414***	***1.416***	***1.454***	***1.485***	***1.473***
O6-C1	**V**	**1.413**	**1.418**	**1.417**	**1.414**	**1.421**
	V	***1.412***	***1.412***	***1.428***	***1.447***	***1.417***

[a]See Table 2 for notation.

into UDP-glucose (Candy 1980). Microbiological oxidation of the CH_2OH group of α-D-galactose provides galacturonic acid which essentially inhibits progress of atherosclerosis (Parikka et al. 2015).

Based on computed values of heat of formation, one could note that the α-anomer was more stable than the β-anomer independently of applied SMF flux density. However, as shown by changes of dipole moment (Table 4), the β-anomer was more po-

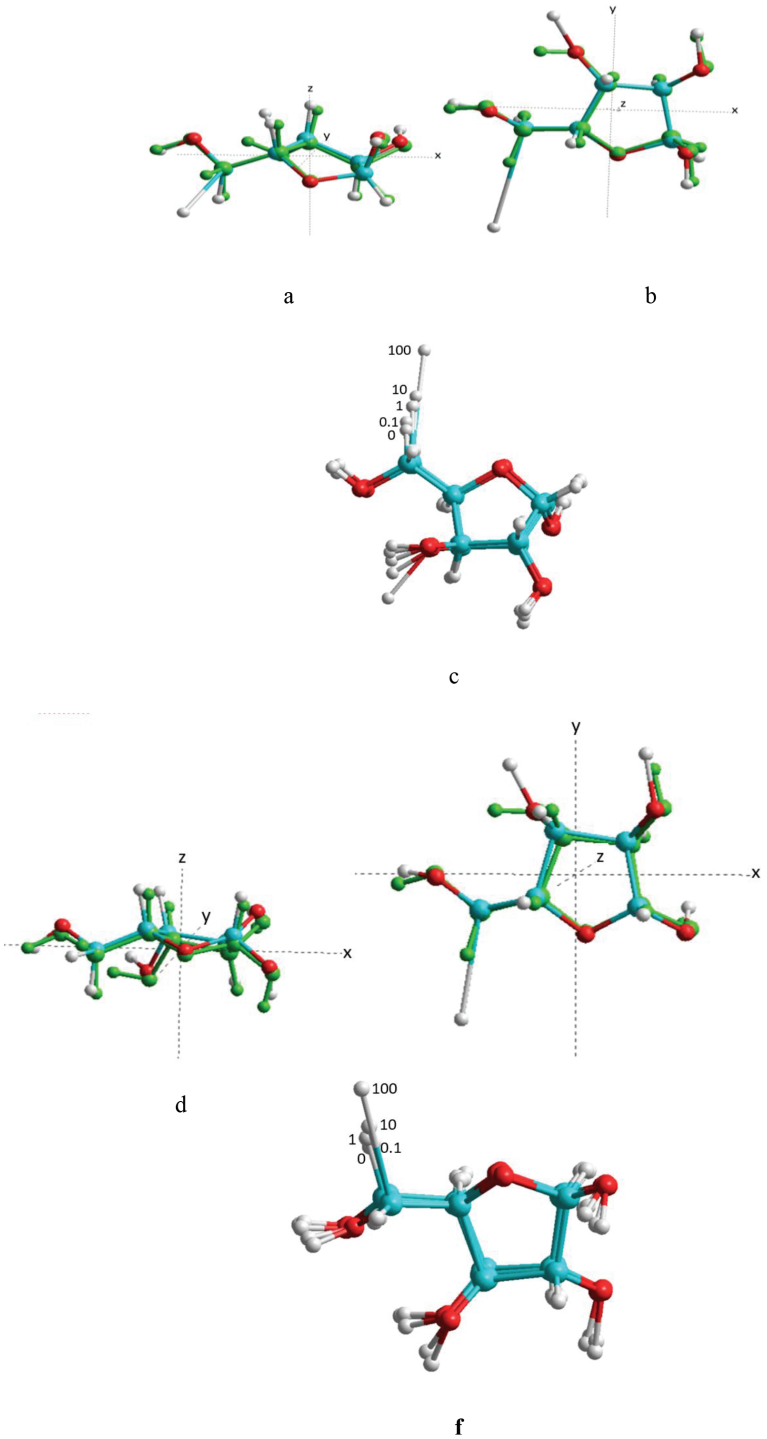

Figure. 10. Simplified visualisation of the effect of SMF upon conformation and bond length of α-D- and β-D-xylofuranose anomers (**a–c** and **d–f** respectively), situated in the Cartesian system (see Fig. 2 for notation).

larised with an increase in the flux density. As in anomers of D-glucose, the charge density at particular atoms irregularly varied with increasing flux density. In contrast to anomers of D-glucose, in anomers of D-galactose, the negative charge concentrated at the O7, C5 and C4 atoms and SMF flux density turned it more negative. The negative charge also concentrated at the C2-H14 atom bound to it (Table 5). The positive charge density was noted at the C3 and C1 atoms, as well as the H15 and H13 atoms bound to them, respectively. These effects generated an increase in the corresponding bond lengths (Table 5).

Due to an increase in the positive charge at the anomeric C6 atom, one could assume a facilitating role of SMF in formation of galactoso-1- phosphate. In addition, the effect of SMF upon the charge density suggested favouring oxidation of D-galactose into galacturonic acid.

Particular attention should be paid to the C5, C6 and H19 atoms. SMF remarkably changed their charge distribution. The negative charge shifted to the C5 and H19 atoms, whereas the C6 atom lost this charge to a considerable extent. The strongest influence was evoked by SMF upon the bonds orientated under 45° to the field strength lines, that is, to the x-axis. Extremal elongation was observed for the C6-H19 and O10-H22 bonds (Table 6). Simultaneously, the C6-H18 bond distinctly shortened. It should be underlined that both H18 and H19 were twin atoms bound to the C6 atom. Thus, observed differences could not originate from different intramolecular electronic interactions and completely different situations by those atoms with respect to the SMF line should be responsible for it.

Unlike in D-glucose, the positive charge density at the C1 atom decreased with an increase in the flux density. Thus, reactions with any Lewis base would be obstructed. Simultaneously, the flux density up to 0.1 AFU increased the negative charge density at the C6 atom. It would favour phosphorylation at the vicinal hydroxyl group. However, higher flux densities turned the charge density at that atom to positive. Thus, the increase in the charge density with the flux density inhibited that reaction.

The susceptibility of D-galactose to the ring opening and to the Maillard reaction depended on its anomer. The C1-O8 bond in the α-anomer varied irregularly with the flux density but, generally, the susceptibility of that anomer to the ring opening was low. That bond in the β-anomer regularly decreased with an increase in the applied flux density. Simultaneously, the O8-H20 bond was shortened in the α-anomer and elongated in the β-anomer (Table 6).

Data shown in Table 6 allowed the visualisation of the effect of SMF upon anomers of D-galactose. Structures in Fig. 6 demonstrate a slight effect of SMF upon the conformation of both anomers and significant effect upon the bond lengths of some peripheral C-H bonds. They were the C6-H18 and O10-H22 bonds. An increasing flux density generated a considerable negative charge density at the H22 atom making the C6-H18 bond relatively slightly polarised. Therefore, that bond was capable of interaction with the electrons of that bond with SMF. In the O10-H22 bond, both its partners carried negative charge. This effect and its origin was the same as that observed in D-glucose anomers.

D-Fructose

D-Fructose, a ketohexose, is a typical monosaccharide of a floral provenance. In the free form, it resides in fruits, honey and flower nectar. In a bound form, it can be found in several di-, oligo- and polysaccharides, for instance, sucrose, raffinose and inulin, respectively. Its presence in the organisms of fauna is a consequence of consumption of plant food. In mammals, free fructose is found in their semen (Maton et al. 1993; Tomasik 1997; Campbell et al. 2006; Tomasik 2007a; Tomasik 2007b; Heldt and Piechulla 2010; Keung and Mehta 2015; Churuangsuk et al. 2018; Reynolds et al. 2019). Humans metabolise D-fructose almost entirely in the liver, where it is directed towards replenishment of liver glycogen and triglyceride synthesis. In muscles and fat tissues, D-fructose metabolism is initiated by phosphorylation with hexokinase at the O11 atom, turning it into fructose-1-phosphate. The latter enters the glycolysis pathway. In the liver, the metabolism of D-fructose is initiated by fructokinase which forms fructose-1-phosphtate engaging the O10 atoms, respectively (Maton et al. 1993; Tomasik 1997; Hames and Hooper 2004; Campbell et al. 2006; ; Tomasik 2007a; Tomasik 2007b; Heldt and Piechulla 2010; Keung and Mehta 2015; Churuangsuk et al. 2018; Reynolds et al. 2019).

Alcohol fermentation and the Maillard browning reaction are other enzymatic processes common for D-fructose. In the Maillard reaction, the anomeric C1 carbon atom is first engaged (Grandhee and Monnier 1991).

D-Fructose resides in four mutually fast interconverting structures, including α-D-fructopyranose (α-Fru*p*), β-D-fructopyranose (β-Fru*p*), α-D-fructofuranose (α-Fru*f*) and β- D-fructofuranose (β-D-Fru*f*) (Fig. 3). Computations of the heat formation (Table 7) pointed to α-D-Fru*f* and α-D-Fru*p* being the most and least stable, respectively, amongst the four anomers taken into account (Fig. 3). Applying SMF of 0.1 AFU, the flux density did not change their positions in this group. At 1 AFU, based on that criterion, β-D-Fru*f* became the most stable, but a further increase in the flux density returned α-D-Fru*f* to the position of the most stable anomer. α-D-Fru*p* holds the position of the least stable anomer at SMF up to 10 AFU. At 100 AFU, β-D-Fru*p* became the least stable. The dipole moment of particular anomers also changed with an increase in the applied flux density. However, these changes were in no simple relationship to the stability of particular anomers. It suggested deformation of their initial structure by polarisation of particular bonds. They could also result from departure from their initial situation in the Cartesian system. This was confirmed by computed changes of charge density and bond lengths (Tables 8–11). Inspection of Table 8 showed that, in α- and β-D-fructopyranoses, the negative charge density essential for the phosphorylation reaction at the O12 atom was lower in the α-anomer and it fairly linearly decreased against increasing flux density. Thus, that anomer should be more reactive than the β-anomer. The Maillard reaction required the positive charge density at the C1 atom. Without SMF, the β-anomer showed a more positive charge at that atom. It decreased against increasing flux density. The α-anomer carried considerably lower positive charge density which additionally decreased against the flux density up to 10 AFU and then increased regularly up to over twice at 100 AFU.

The strongest changes in the electron density occurred at the C1, O12α, H13α, H22β and H24β atoms. Thus, both anomers are clearly distinguished from one another.

Structural deformations of the α- and β-D-fructopyranose molecules in SMF (Table 9 and Fig. 6) resembled those observed for D-glucose and D-galactose anomers. Considerable elongations were observed for the C1-H13, O11-H22 bonds and C6-H19α bonds, whereas the twin C6-H18 bond was only slightly shortened. It was another illustration of the importance of the position of the bonds with respect to the SMF field.

In the case of D-fructofuranoses, comparison of the negative charge density (Table 10) at the O12 and O11 atoms being potentially the reaction sites for the phosphorylation suggested that the β-anomer should react more readily than the α-anomer. An increase in the SMF flux density was not beneficial for this reaction as the value of the charge density at these atoms turned less negative. The positive charge density at the C4 and C1 atoms, being the potential reaction site for the Maillard reaction, were higher in the β-anomer and only slightly decreased with increasing AFU. SMF at 100 AFU generated an essential increase in the positive charge density at the C1β, O9β, O12α and H21α atoms. At the same time, that charge decreased at the C2α, C5β, H17α, H24α and particularly at the H20β atom.

Anomers of D-fructofuranoses were less susceptible to structural deformations evoked by SMF (Table 11 and Fig. 8). In the α-anomer, the O12-H24, O9-H22 and C5-H17 bonds were longer and that effect was noticeable just at 100 AFU. The β-anomer was deformed chiefly by elongation of the O9-H22, C1-C2 and O8-H20β bonds. Untypically, the ring was also deformed by the elongation of the C2-C1 bond.

D-Xylose

D-xylose, aldopentose, is a mono-sugar residing almost exclusively in plants. As a component of hemicelluloses, it constitutes biomass. In the sphere of fauna, D-xylose was also found in some species of Chrysolinina beetles. It co-constituted cardiac glycosides of their defensive glands (David Morgan 2004).

Organisms of fauna receive xylose from their diet. Eukaryotic micro-organisms employ the oxidato-reductase pathway to metabolize D-xylose (Gabaldon et al. 2005). D-xylose is metabolised by humans involving protein xylosyltransferases (XYLT1, XYLT2) which transfer xylose from UDP to a serine in the core protein of proteoglycans (Stoolmiller et al. 1972; Gotting et al. 2000). Mammals metabolise D-xylose with D-xyloisomerase (Ding et al. 2009; Huntley and Patience 2018). Recently, a highly efficient low-temperature, atmospheric-pressure enzymatic process of the hydrogen production from D-xylose was presented. It involved thirteen enzymes, including a novel polyphosphate xylulokinase (Del Campo et al. 2013). In another technically important reaction, D-xylose is used for production of furfural, a precursor for synthetic polymers and to tetrahydrofuran (Hoydonckx et al. 2007). In the initial step, hemicellulose is hydrolysed in an acid-catalysed process (Binder et al. 2010; Millán et al. 2019). That process starts from the protonation of the D-xylopyranose molecule at the O8 atom.

It was also found that D-xylose could be useful in therapy of COVID-19 (Cheudjeu 2020). The latter interacts with D-xylose significantly stimulating the biosynthesis of sulphated glycosylamineglycans (GAGs), particularly heparan sulphate (HS). GAGs, especially HS and D-xylose interact with oral non-steroidal anti-inflammatory drugs, active in lung infections.

D-Xylose resides in the form of α- and β-xylopyranoses (Xyl*p*) (a and b), as well as α- and β-xylofuranoses (Xyl*f*) (c and d) (Fig.4).

The heat of formation criterion pointed to β-D-xylopyranose as the most stable amongst four anomers of D-xylose (Table 12). It is distinguished from other anomers with a considerably low dipole moment. The increase in the SMF flux density regularly increased the dipole moment of all anomers and, at the same time, destabilised them in terms of their heat of formation values. In both D-xylopyranoses, the metabolic reactions should be promoted by the high positive charge density at the O6 atom and low negative charge density at the O8 and O9 atoms. Data in Table 13 showed that the influence of SMF upon the O6, O9 and O8 atoms was negligible, noticeable and strong, respectively. A considerable increase in the positive charge density took place at the C1α, C5 and O8 atoms, whereas its decrease was observed at the C2 and H18β atoms. The SMF flux density promoted reactivity at the C1, especially the C1α atom, slightly promoted reactions at the O9 atom and strongly increased the reactivity of the O8 atom. Taking these arguments under consideration, the α-anomer was more reactive at the C1 atom when residing without SMF and, in SMF, the β-anomer reacted more readily. The reactivity at the O8 atom in the β-anomer was slightly higher when SMF was applied and the reactivity at the O7 atom in the α-anomer was definitely higher.

As shown in Table 14 and Fig. 9, only the O8-H18 bond suffered considerable elongation in SMF. Less intense elongation was observed at the C4-H14 and C5-H15 bonds in both anomers. That effect was in line with the preference for the elongation of the bonds orientated under approximately 45° with respect to the x-axis.

Metabolic processes in D-xylofuranose molecules involved the C1 and O10 atoms. The highly positive and highly negative charge densities, respectively, were beneficial for those reactions. Data in Table 13 showed that, in both anomers, SMF did not influence charge density at the C1 atom. SMF generated a decrease in the negative charge density at the O10 atom. It was particularly noticeable in the α-anomer. It pointed to an inhibition of the reactivity with Lewis acids in these centres. An increase in the positive charge density at the C5α, O9, O10α, H11, H15α and H19 atoms and its decrease at the C4β and H16 atoms confirmed the rule of the importance of 45° orientation of the bonds with respect to the SMF field. Data in Table 16 and Fig. 10 showed that, in both anomers, the C5-H15 bond reacted intensively to an increase in the flux density and the response from the C4-H14 and O9-H19α bonds was weaker.

Comparison of the relevant data for D-xylopyranoses and D-xylofuranoses revealed that pyranose anomers metabolise more readily.

The SMF flux densities ranging from 100 to 10 000 T (0.1 to 100 AFU) employed in performed computations were very high. Experiments performed by Nakamura et al. Takeyama (Nakamura et al. 2018) with SMF of 1200 T (1.2 AFU) resulted in a

destruction of the generators within few microseconds. The pulse electromagnet constructed in 2012 at Los Alamos Laboratories remained stable, but producing a field with an intensity of only 100.75 T (approx. 0.1 AFU) (Nguyen et al. 2016). Therefore, only insignificant effects evoked by SMF of flux density of 0.1–100T (0.0001–0.1 AFU) upon carbohydrates could be anticipated in a real life.

Conclusions

Performed numerical simulations showed the specific influence of static magnetic field (SMF) upon equilibrium constants between particular anomers of the saccharides under study. Their susceptibility to such enzymatic reactions essential for their metabolism as phosphorylation with ATP at the CH_2OH group, the Entner-Duodoroff metabolic pathway and the Maillard reaction, both also engaging the C1 ring carbon atom in reaction with enzymes and amino acids, is also controlled by SMF.

D-Glucose in SMF takes preferably the α-anomeric form. SMF stimulated its reactivity involving the CH_2OH group and the C1-atom.

D-Galactose in SMF takes preferably the α-anomeric form. The reactivity at the CH_2OH group and C1 atom vary irregularly with an increase of the applied flux density.

D-Fructose in SMF takes preferably the α-D-Fru*f* form and D-xylose under such conditions takes preferably the β-D-Xyl*p* form. Their susceptibility to the reactions important for their metabolism irregularly vary with the applied flux density.

Only insignificant effects evoked by SMF of flux density of 0.1–100T upon carbohydrates could be anticipated in a real life.

References

Bao S, Guo W (2021) Transient heat transfer of superfluid He in nonhomogeneous geometries: Second sound, rarefaction, and thermal layer. Physical Review B 103(13): e134510. https://doi.org/10.1103/PhysRevB.103.134510

Binder JB, Blank JJ, Cefali AV, Raines RT (2010) Synthesis of furfural from xylose and xylan. ChemSusChem 22(11): 1268–1272. https://doi.org/10.1002/cssc.201000181

Campbell NA, Williamson B, Heyden RJ (2006) Biology: Exploring Life. Pearson Prentice Hall, Boston.

Candy DJ (1980) The Biochemistry of Plants. Academic Press, New York.

Carpenter JE, Weinhold F (1988) Analysis of the geometry of the hydroxymethyl radical by the different hybrids for different spins natural bond orbital procedure. Journal of Molecular Structure (Teochem) 139: 41–62. https://doi.org/10.1016/0166-1280(88)80248-3

Charistos ND, Muñoz-Castro A (2019) Double aromaticity of the B-40 fullerene: Induced magnetic field analysis of pi and sigma delocalization in the boron cavernous structure. Physical Chemistry Chemical Physics 21(36): 20232–20238. https://doi.org/10.1039/C9CP04223G

Cheudjeu A (2020) Correlation of D-xylose with severity and morbidity-related factors of COVID-19 and possible therapeutic use of D-xylose and antibiotics for COVID-19. Life Sciences 260: e118335. https://doi.org/10.1016/j.lfs.2020.118335

Churuangsuk C, Kherouf M, Combet E, Lean M (2018) Low-carbohydrate diets for overweight and obesity: A systematic review of the systematic reviews. Obesity Revs. Systematic Reviews 19: 1700–1718. https://doi.org/10.1111/obr.12744

Ciesielski W, Girek T, Oszczęda Z, Soroka JA, Tomasik P (2021) Towards recognizing mechanisms of effects evoked in living organisms by static magnetic field. Numerically simulated effects of the static magnetic field upon simple inorganic molecules. F1000 Research 10: e611. https://doi.org/10.12688/f1000research.54436.1

Ciesielski W, Girek T, Oszczeda Z, Soroka JA, Tomasik P (2022) Potential risk resulting from the influence of static magnetic field upon living organisms. Numerically simulated effects of the static magnetic field upon simple alkanols. BioRisk 18: 35–55. https://doi.org/10.3897/biorisk.18.76997

Committee to Assess the Current Status and Future Direction of High Magnetic Field Science in the United States, Board on Physics and Astronomy (2013) High Magnetic Field Science and Its Application in the United States; Current Status and Future Directions. Natl. Res. Council, National Acad., Washington, D.C.

Conway T (1992) The Entner-Doudoroff pathway: History, physiology and molecular biology. Microbiological Reviews 103: 1–28. https://doi.org/10.1111/j.1574-6968.1992.tb05822.x

David Morgan E (2004) Biosynthesis in Insects. Royal Society of Chemistry Publ, London, 112 pp.

Del Campo JSM, Rollin J, Myung S, Chun Y, Chandrayan S, Patino R, Adams MWW, Zhang PY-H (2013) High-yield production of dihydrogen from xylose by using a synthetic enzyme cascade in a cell-free system. Angewandte Chemie International Edition 52(17): 4587–4590. https://doi.org/10.1002/anie.201300766

Ding M, Teng Y, Yin Q, Chen W, Zhao F (2009) Identification, expression, and characterization of the highly conserved D-xyloseisomerase in animals. Acta Biochimica et Biophysica Sinica 41(2): 116–122. https://doi.org/10.1093/abbs/gmn013

Domb AJ, Kost J, Wiseman D (2019) Handbook of Biodegradable Polymers. CRC Press, Boca Raton.

Facundo Ruiz CA-A, Martínez-Mendoza JR, Terrones H (2005) Infrared and Raman spectra, conformational stability, *ab initio* calculations of structure, and vibrational assignment of α and β glucose. Journal of Molecular Structure (Teochem) 714(2–3): 143–146. https://doi.org/10.1016/j.theochem.2004.09.041

Farberovich OV, Mazalova VL (2016) Ultrafast quantum spin-state switching in the Co-ctaethylporphyrin molecular magnet with a terahertz pulsed magnetic field. Journal of Magnetism and Magnetic Materials 405: 169–173. https://doi.org/10.1016/j.jmmm.2015.12.038

Frisch MJ, Pople JA, Binkley JS (1984) Self-consistent molecular orbital methods. 25. Supplementary functions for Gaussian basis sets. The Journal of Chemical Physics 80(7): 3265–3269. https://doi.org/10.1063/1.447079

Frisch MJ, Trucks GW, Schlegel HB, et al. (2016) Gaussian 09, Revision A.02, Wallingford CT, Gaussian Inc.

Froimowitz M (1993) HyperChem: A software package for computational chemistry and molecular modeling. BioTechniques 14: 1010–1013.

Gabaldon T, Rainey D, Huynen MA (2005) Tracing the evolution of a large protein complex in the eukaryotes, NADH: Ubiquinone oxidoreductase (Complex I). Journal of Molecular Biology 348(4): 857–870. https://doi.org/10.1016/j.jmb.2005.02.067

Glendening ED, Reed AE, Carpenter JE (1987) Extension of Lewis structure concepts to open-shell and excited-state molecular species, NBO Version 3.1, Ph.D. thesis, University of Wisconsin, Madison.

Gotting C, Kuhn J, Zahn R, Brinkmann T, Kleesiek K (2000) Molecular cloning and expression of human UDP-d-Xylose: Proteoglycan core protein beta-d-xylosyltransferase and its first isoform XT-II. Journal of Molecular Biology 304(4): 517–528. https://doi.org/10.1006/jmbi.2000.4261

Grandhee SK, Monnier VM (1991) Mechanism of formation of the Maillard protein cross-link pentosidine. The Journal of Biological Chemistry 266(18): 11649–11653. https://doi.org/10.1016/S0021-9258(18)99006-X

Hames BD, Hooper NM (2004) Short lectures, Biochemistry. PWN Scientific Editorial Board, Warsaw. [in Polish]

Hamza A-SHA, Shaher SA, Mohmoud A, Ghania SM (2002) Environmental pollution by magnetic field associated with power transmission lines. Energy Conversion and Management 43(17): 2443–2452. https://doi.org/10.1016/S0196-8904(01)00173-X

Heinrich PC, Mueller M, Graeve L (2014) Löffler/Petrides Biochemie und Pathobiochemie. Springer-Verlag, Berlin. https://doi.org/10.1007/978-3-642-17972-3

Heldt H-W, Piechulla B (2010) Plant Biochemistry, 4th edn. Academic Press, Cambridge MA, US.

Hoydonckx HE, Van Rhijn WM, Van Rhijn W, De Vos DE, Jacobs PA (2007) Furfural and its derivatives. Ullmann's Encyclopaedia of Industrial Chemistry. Wiley-VCH, Weinheim. https://doi.org/10.1002/14356007.a12_119.pub2

Huntley NF, Patience JF (2018) Xylose: Absorption, fermentation, and post-absorptive metabolism in the pig. Journal of Animal Science and Biotechnology 9(1): e4. https://doi.org/10.1186/s40104-017-0226-9

Keung PC, Mehta CBM (2015) Handbook of Food Chemistry. Springer, Berlin/Heidelberg. https://doi.org/10.1007/978-3-642-36605-5_34

Largeaud F, Kokoh KB, Beden B, Lamy C (1995) On the electrochemical reactivity of anomers: Electrocatalytic oxidation of α- and β-D-glucose on platinum electrodes in acid and basic media. Journal of Electroanalytical Chemistry (Lausanne, Switzerland) 397(1–2): 261–269. https://doi.org/10.1016/0022-0728(95)04139-8

Marchand N, Lienard P, Siehl H, Izato H (2014) Applications of molecular simulation software SCIGRESS in industry and university. Fujitsu Scientific and Technical Journal 50(3): 46–51.

Maton A, Hopkins J, McLaughlin CW, Johnson S, Warner MQ, LaHart D, Wright JD (1993) Human Biology and Health. Prentice Hall, New Jersey.

Millán GG, Hellsten S, King AWT, Pokki J-P, Llorca J, Sixta H (2019) A comparative study of water-immiscible organic solvents in the production of furfural from xylose and birch

hydrolysate. Journal of Industrial and Engineering Chemistry 72: 354–363. https://doi.org/10.1016/j.jiec.2018.12.037

Nakamura D, Ikeda A, Sawabe H, Matsuda YH, Sakeyama S (2018) Record indoor magnetic field of 1200 T generated by electromagnetic flux-compression. The Review of Scientific Instruments 89(9): e095106. https://doi.org/10.1063/1.5044557

Nguyen DN, Michel J, Mielke CH (2016) Status and development of pulse magnets at the NHMFL pulsed field facility. IEEE Transactions on Applied Superconductivity 26(4): e1. https://doi.org/10.1109/TASC.2016.2515982

Parikka K, Master E, Tenkanen M (2015) Oxidation with galactose oxidase: Multifunctional enzymatic catalysis. Journal of Molecular Catalysis. B, Enzymatic 120: 47–59. https://doi.org/10.1016/j.molcatb.2015.06.006

Rankovic V, Radulovic J (2009) Environmental pollution by magnetic field around power lines. International Journal of Qualitative Research 3(3): 1–6.

Reynolds A, Mann J, Cummings J, Winter N, Mete E, Morenga L (2019) Carbohydrate quality and human health: A series of systematic reviews and meta-analyses. Lancet (Review) 393(10170): 434–445. https://doi.org/10.1016/S0140-6736(18)31809-9

Sell DR, Monnier VM (1989) Structure elucidation of a senescence cross-link from human extracellular matrix. Implication of pentoses in the aging process. The Journal of Biological Chemistry 264(36): 21597–21602. https://doi.org/10.1016/S0021-9258(20)88225-8

Stoolmiller AC, Horwitz AL, Dorfman A, Kennedy Jr JP (1972) Biosynthesis of the chondroitin sulfate proteoglycan. Purification and properties of xylosyltransferase. The Journal of Biological Chemistry 247(11): 3525–3532. https://doi.org/10.1016/S0021-9258(19)45172-7

Tang Y, Guo W, Lvov W, Pomyalov A (2021) Eulerian and Lagrangian second-order statistics of superfluid He grid turbulence. Physical Review B 103(14): e144506. https://doi.org/10.1103/PhysRevB.103.144506

Tomasik P (1997) Saccharides. In: Sikorski ZE (Ed.) Chemical and Functional Properties of Food Components, Ch. 4. Technomic Publ. Co. Inc., Lancaster – Basil.

Tomasik P (2007) Saccharides in food, Structure and transformations. In: Sikorski ZR (Ed.) Food Chemistry, Ch. 1. WNT, Warsaw.

Tomasik P (2007) Functional properties of saccharides. In: Sikorski ZR (Ed.) Food Chemistry, Ch. 2. WNT, Warsaw.

World Health Organization (2019) Model list of essential medicines: 21st list. Geneva, hdl:10665/325771